NTNU
Norwegian University of
Science and Technology

Model Development for Optimal Operation of the District Heating Facilities of Fortum Oslo Varme

Using Genetic Algorithm, Recurrent Neural Network and Multiple Linear Regression

Marius Jean Bischof Hagalid

Master of Energy and Environmental Engineering
Submission date: July 2018
Supervisor: Natasa Nord, EPT

Norwegian University of Science and Technology
Department of Energy and Process Engineering

NTNU
Norwegian University
of Science and Technology

Department of Energy
and Process Engineering

EPT-M-2018-35

MASTER THESIS

for

Student Marius Jean Bischof Hagalid

Spring 2018

Model development for automatic control of the plant at Hafslund Heating regarding reliability and optimal operation

Utvikling av modeller for automatisk styring av anleggene i Hafslund Varme med hensyn til pålitelighet og optimal drift

Background and objective

In most of current district heating systems, production planning is based on historical data, weather forecasts, fuel prices, and environmental priorities. Utilization of different operation data and real-time management have been used for plant control to a limited extent. Generally, a recommended schedule for the production planning is developed for one week at a time for the operator at the operating center. The plan is updated daily with regard to weather forecasts. Operators start and stop installations manually as needed based on observation of pressure differences at strategic locations in the network. Among the units in operation, operators have to select at least one unit as the control unit, i.e. the load on the boiler is controlled by the differential pressure at the selected locations in the district heating network. It is particularly demanding to be prepared for the night operation before working day with considerable low temperature. In that case, the facilities must be ready to meet the "morning peak" as all commercial buildings and households are using high heat rate. In the district heating system in Oslo, it is installed approx. 1000 MW capacity divided into 40 boilers with different energy carriers. The energy carriers range from waste, heat pumps from sewage, power, wood pellets, industrial waste, bio liquids, biodiesel, LNG, and some fossil oil. In order to solve the above challenges in the operation of district heating systems and increase the reliability of heat supply, it is important to utilize better and smarter operating data and data on heat demand. In order to increase reliability and improve economy, it is also important to look at the possibility of expanding thermal storage facilities. The student has collected operational data during this project assignment. The student has started to learn some methods for data processing. Some of the data were processed by using different methods for data processing. The assignment is linked to the company Hafslund Varme and a prestigious research project, UnDID, on smart district heating. During the master assignment, the student should also establish collaboration with the students at OsloMet about control and optimization.

The aim of the assignment is to develop the control logics and strategies for automated management models for the operation of district heating in Oslo. These strategies should utilized in an efficient way available operation data.

The following tasks are to be considered:

1. Literature study on district heating technology as well as examples of optimization of district heating operations. Literature studies should deal with statistical methods of data processing relevant to the assignment.
2. Collect and organize data on the district heating system at Hafslund District Heating. Present technical data about the plant.
3. Collect and organize historical operating data from Hafslund Heating. It is beneficial to have data over several years.
4. Use literature study and theoretical basis (thermodynamic and mathematical) to develop a basis for better management of the district heating system. Define relevant optimization issues using mathematical theory of optimization or practical approach.
5. Test few methods for data processing to find a good and efficient heat load prediction method. Present the method quality based on the model error.
6. Test one or few methods for the plants optimization. Present hourly, montly, and annual data. Post-process the results to enable verification of the method.
7. Perform sensitivity analysis of the automatic control models.
8. Organizing and presenting results.
9. Develop material for a draft conference or journal paper.

-- " --

Within 14 days of receiving the written text on the master thesis, the candidate shall submit a research plan for his project to the department.

When the thesis is evaluated, emphasis is put on processing of the results, and that they are presented in tabular and/or graphic form in a clear manner, and that they are analyzed carefully.

The thesis should be formulated as a research report with summary both in English and Norwegian, conclusion, literature references, table of contents etc. During the preparation of the text, the candidate should make an effort to produce a well-structured and easily readable report. In order to ease the evaluation of the thesis, it is important that the cross-references are correct. In the making of the report, strong emphasis should be placed on both a thorough discussion of the results and an orderly presentation.

The candidate is requested to initiate and keep close contact with his/her academic supervisor(s) throughout the working period. The candidate must follow the rules and regulations of NTNU as well as passive directions given by the Department of Energy and Process Engineering.

Risk assessment of the candidate's work shall be carried out according to the department's procedures. The risk assessment must be documented and included as part of the final report. Events related to the candidate's work adversely affecting the health, safety or security, must be documented and included as part of the final report. If the documentation on risk assessment represents a large number of pages, the full version is to be submitted electronically to the supervisor and an excerpt is included in the report.

Pursuant to "Regulations concerning the supplementary provisions to the technology study program/Master of Science" at NTNU §20, the Department reserves the permission to utilize all the results and data for teaching and research purposes as well as in future publications.

The final report is to be submitted digitally in DAIM. An executive summary of the thesis including title, student's name, supervisor's name, year, department name, and NTNU's logo and name, shall be submitted to the department as a separate pdf file. Based on an agreement with the supervisor, the final report and other material and documents may be given to the supervisor in digital format.

☐ Work to be done in lab (Water power lab, Fluids engineering lab, Thermal engineering lab)
☐ Field work

Department of Energy and Process Engineering, 15. January 2018

Natasa Nord

Natasa Nord
Academic Supervisor

Research Advisor:
Knut Inderhaug, Hafslund Varme AS, Knut.Inderhaug@hafslund.no

]

Preface

This is a master thesis written at Department of Energy and Process Engineering, NTNU. It is written in cooperation with Fortum Oslo Varme during spring of 2018. The thesis is part of the research project UnDiD, *Understanding behavior of District heating systems, Integrating Distributed sources.*

I want to thank my supervisor, associate professor Natasa Nord, for valuable support through the semester. She helped with guiding the project in the right direction.

I also want to thank Fortum Oslo Varme for their cooperation and support. I received help from Øyvind Nilsen, Karine Huuse and in particular Birgitte Johannesen who was my supervisor. She was very helpful with collection of data, and provided good advice from an industry perspective. Her feedback on the first chapters of the thesis was valuable as well.

Summary

Recent development in the energy sector in Norway has made district heating increasingly relevant. In particular, the increased demand for electric power, has contributed to make district heating more important.

A well known problem in district heating, is operational optimization. In this thesis, the problem is investigated on the basis of the Fortum Oslo Varme's system, which consists of more than 40 boilers. All data used in the thesis is gathered from Fortum's data system.

Another prominent theme in district heating, is the possibility for building thermal energy storages. Methods which can calculate the profitability of investing in thermal energy storages are necessary.

To solve the issue of operational optimization, models for predicting future heat load demand are necessary. Two such models were developed, the best of which were able to predict the heat load demand with an average error of 7.6% in the years 2013 and 2014.

Additionally, a model for operational optimization was developed. It can be run both with and without an accumulator tank, so that the operational cost can be compared, and investment decisions can be taken. It was found that a system with an accumulator tank can save 1.3 million NOK yearly, based on simulations performed on data from 2016. The investment in a tank is not profitable, given an assumed cost of 39 million NOK.

It must, however, be taken into account that potential savings will vary between years. The simulations also build on some assumptions about the district heating system, and the thermal energy storage. Since the optimization model is based on randomness, two consecutive runs would not give the same result. Therefore, additional simulations are required to verify the results.

Sammendrag

Utviklingen innenfor energisektoren i Norge de siste årene har gjort fjernvarme stadig mer aktuelt. Spesielt den økte konkurransen for elkraft, har vært med på å øke viktigheten av fjernvarme.

Et kjent problem innen fjernvarme, er optimalisering av driften. Det er viktig å drifte ethvert anlegg med lavest mulig utgifter, slik at det er konkurransedyktig. I denne oppgaven utforskes problemstillingen på basis av anlegget til Fortum Oslo Varme, som består av over 40 kjeler. All data som er brukt i oppgaven, er hentet fra Fortums datasystem.

Et annet aktuelt tema innen fjernvarmebransjen, er muligheten for å bygge termiske energilager. Det er et behov for metoder til å beregne om det er økonomisk lønnsomt å investere i slike energilager.

For å løse problemet med å drifte et anlegg optimalt, trenger man modeller som kan forutsi fremtidig lastbehov. Det har blitt utviklet to modeller som forutsier lastbehov i fjernvarmenettet. Den mest presise av disse klarte å forutsi lastbehovet med en gjennomsnittlig feil på 7,6% for årene 2013 og 2014.

I tillegg er det blitt utviklet en modell som optimaliserer driften av anlegget, gitt at man kjenner fremtidig lastbehov. Denne modellen kan kjøres med eller uten akkumulatortank, slik at man kan sammenligne driftskostnadene, og avgjøre om det er en lønnsom investering. Det ble funnet ut at et anlegg med akkumulatortank kan spare 1,3 millioner kroner årlig, basert på simuleringer gjort på data fra 2016. Dette er ikke nok til å kunne rettferdiggjøre den antatte investeringskostnaden på 39 millioner kroner.

Det må imidlertid tas forbehold om at årlige besparelser ved investering i akkumulatortank vil variere fra år til år. Simuleringene bygger også på antagelser om anlegget og et eventuelt termisk energilager. I tillegg er det usikkerhet knyttet til optimaliseringsmodellen, siden denne er bygget på tilfeldighet, noe som gjør at to påfølgende kjøringer ikke gir samme resultat. Gjentatte simuleringer må derfor gjennomføres for å bekrefte resultatene.

Contents

List of Figures

List of Tables

Chapter 1

Introduction

District Heating (DH) is a flexible system for distribution of energy. It provides opportunity to utilize a mix of energy sources, in order to maximize their advantages, and minimize their drawbacks. Moreover, it provides opportunity to utilize low-grade energy sources that could not have been taken advantage of otherwise. Waste heat from data centers and heat extracted from waste combustion are examples of such sources.

In Norway, the abundance of cheap, environmentally friendly energy from hydropower has traditionally made the competitors somewhat redundant. Electricity has been the dominating carrier of energy for all purposes, including heating. This has been the case even if using high-grade valuable energy, which electricity indeed is, to cover a low-grade exchangeable demand is considered by many to be wasteful.

Following the deregulation of the Norwegian electricity market in 1990, however, electricity prices have been increasing (Aanensen and Fedoryshyn, 2014, p. 8). There has been development of the Norway to Europe cross-border electricity lines. As of 2015 Norway had a transmission capacity of about 6000 MW, excluding planned lines to Germany and Great Britain (Rosvold and Vinjar, 2015). Increased export of electricity, has naturally contributed to increase the scarcity of the resource on a national level.

In recent years, Norwegian tax laws has been another factor to make electricity scarcer. Tax benefits provided to el-car owners by the Norwegian government has made el-cars increasingly more common. As electricity gets a new field of application, new buyers start competing for an already scarce resource.

By 2015, 62% of the potential for hydropower was already developed (NVE, 2015). Since hydropower is not infinitely expandable, a redistribution of the available electricity becomes necessary. Non el-specific purposes will naturally give way in favor of those that are. DH can replace electricity in covering the demand for domestic heating, as it is not an el-specific demand. This has the added benefit of being able to utilize the low-grade energy sources like waste and waste heat. All of this makes DH a very viable option for Norway going forward.

1.1 Background

1.1.1 Operations Planning

A DH grid typically consist of a number of boilers utilizing different energy sources. These can be spread out geographically and are connected to each other and consumer substations by insulated pipes in the ground. Water flowing through these pipes is the medium of energy transport. Cold water is heated by the boilers, and then flows to the substations where it releases heat to the consumers.

The operation of a DH grid is however a complex undertaking, consisting of a number of tasks and decisions. Operation decisions being made, directly affect the cost of operation, and it is therefore crucially important to make close to optimal decisions. If a DH grid is operated suboptimally, the profitability of the operation decreases, weakening DH's competitiveness compared to other solutions. The direct competitors to DH include electricity based solutions and local solutions. If it is cheaper for the consumer to employ local solutions, like local heat pumps or stoves, DH may be competed out of the market.

With this in mind, let us review the current situation of the DH business. In general there will be variations to how each actor in DH performs specific tasks, but most DH businesses employ a combination of IT resources and human resources in day to day operation planning.

For example, it is possible to use IT tools to make optimized planning schedules and employ production operators to handle the operation of the boilers. Computer generated production plans will sometimes also have to be reviewed by qualified personnel in order to ensure their optimality.

This interaction between personnel and computers can be exemplified by the way load forecasting is performed at Fortum Oslo Varme. Load forecasting is initially performed by a computer program, which makes predictions based on historical data. However, operating staff have experienced that these predictions are generally not accurate enough, so the staff has to edit the predictions yielded by the model to make them more accurate.

Employing personnel to perform specific tasks and decisions are sometimes, depending on the task, more expensive than using automatic models. If utilizing computer models to a larger degree simultaneously enables the business to cut back on staff, there is an added economic incentive to do so. By creating more accurate and reliable models, one could potentially cut back on staff, reducing expenses in the form of wages.

As mentioned, operating a DH system involves a number of separate tasks. In the following, some relevant operations scheduling tasks will be presented.

Unit Commitment

Unit commitment is a form of short- or long-term production scheduling. It essentially consists of determining which units shall be turned on at every given point in time during the planning horizon. The criteria for deciding which units should be active, is minimization of the operation cost. Often, the environmental impact of operation is considered as well.

A prerequisite for deciding the unit commitment, is to have an accurate prediction of the required Heat Load (HL). Another is to know the specific price of the energy carriers and the technical specifications for each boiler.

With the prerequisite knowledge, it is possible to make enlightened decisions regarding the unit commitment. By selecting the optimal combination of on/off statuses at each hour during the planning horizon, one can minimize the operation cost. Finding the optimal schedule in a system with tens of boiler units is, however, a very challenging task that require sophisticated search techniques.

The prerequisite of knowing energy prizes and HL demand ahead of time puts some limitations on how far ahead it is sensible to schedule. In the day ahead market for electricity, 12:00 CET is the deadline for submitting bids for power which will be delivered the following day. Hourly prices are typically announced to the market at 12:42 CET or later (Nord Pool, a). Another limitation is the accuracy of weather forecasts. Accurate meteorological forecasts are necessary to predict the HL demand, but the uncertainty of forecasts increases with the forecasting horizon.

The uncertainty of forecasts and electricity prices, makes long-term scheduling less feasible than short-term scheduling. A longer scheduling horizon also increases the demand for processing power and/or processing time. Conveniently, long-term planning is not necessary in day to day operation, since HL demand vary according to daily patterns.

Load Forecasting

Load forecasting is the process of predicting future HL demand based on a number of parameters. Understanding which parameters impact the demand is part of the challenge. Naturally, consumer patterns and weather play an important role (Dotzauer, 2002, p. 1). Faults in the weather forecast will then carry over to the demand forecast.

To find patterns of how the parameters affect HL demand, studying historical HL demand is very useful. Analyzing how the parameters have affected demand in the past, is helpful in discovering the correlation between the observed values. When performing forecasts, one utilizes the established correlation to determine the future demand.

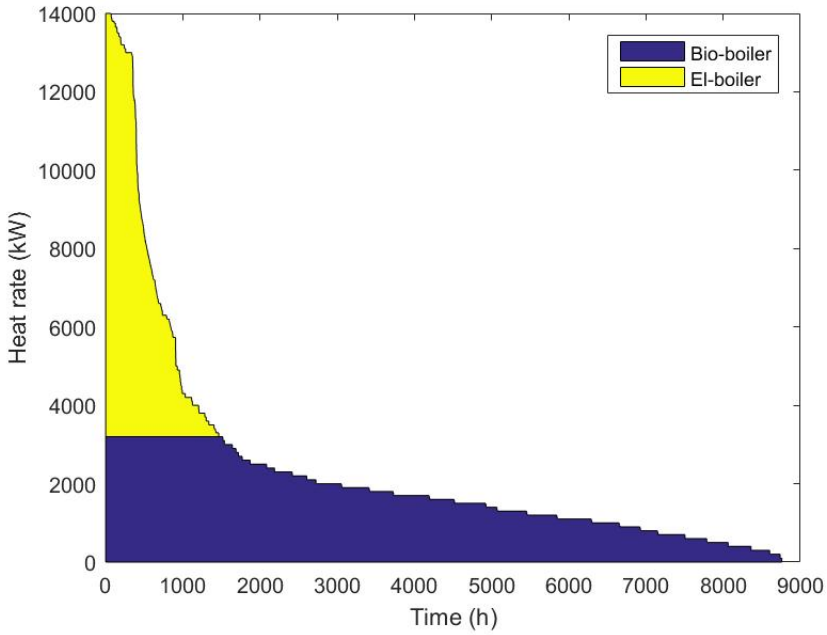

Figure 1.1: Example of a heat load profile

1.1.2 Investment in Thermal Energy Storages

A DH system consists of boilers with different properties and different purposes. Some boilers have high investment costs and low operation costs. This makes them suitable to cover the base load demand, which is the demand with low absolute value but long duration. These boilers will typically be active throughout the year to fully utilize the investment and save costs on operation. To cover the peak load demand it is cheaper to use boilers with low investment costs and high operation costs.

Figure 1.1 shows an example of a load profile of a DH system, where the distinction between peak load boilers and base load boilers is evident. The system consists of two boilers, where the bio-boiler is assigned to the base load and stays active throughout the year. Only when demand exceeds the generation capacity of the bio-boiler, the el-boiler is activated.

In order to decrease the use of peak boilers, and thereby reducing operation costs, it is possible to invest in a Thermal Energy Storage (TES). A TES can accumulate cheap heat when demand is low, so that this heat can be released when the demand increases, replacing heat from peak boilers.

In recent years, deciding whether to invest in short-term energy storages has been a highly relevant topic to Norwegian DH companies. IT tools have shown to be a good aid in making such decisions.

Statkraft Varme is an example of a company which is currently working on the installation of an accumulator tank at their facility in Trondheim. It can hold 5000 m^3 of 120°C water. When making the decision to invest in the tank, Statkraft employed a simulation tool which showed that the tank would lead to better energy utilization (Graver, 2016).

Fortum Oslo Varme has considered to invest in an accumulator tank for some years, but in the past calculations have shown that it would not be profitable. However, such matters has to be reevaluated continuously, as the DH system changes over time. An updated and more detailed analysis is necessary in order to reevaluate the decision, so that potential profits are not lost. Simulating the DH system in detail over time could enable the company to take a more informed decision.

One way of deciding the profitability of the investment would be to run a unit commitment optimization of the DH system at hand. By optimizing a longer time horizon, for example a year, one would get an estimate of the total operation costs over the year. If the same system is then optimized with an imagined TES installed, one would get a different result for the total operation cost. Comparing the operation costs of the system with and without a TES, it is possible to decide whether the investment is profitable or not. Reviewing the variations in HL demand throughout the year also gives an indication of whether the investment is worthwhile.

1.2 Problem Formulation

This thesis aims to develop models which solves the issue of DH operations scheduling over short time horizons, focusing on the issues discussed in the preceding section. In the following, there is a list of subproblems which are to be solved to achieve this goal.

1. Data Collection

   The first subproblem is to gather and present data about the DH system at hand. The system should be mapped out, including boilers, facilities and the grid. Furthermore, historical data necessary to complete the remaining objectives has to be collected and presented in a well arranged manner.

2. HL Prediction

   Develop multiple models for HL prediction, and evaluate which model provides the best fit. These models must be able to run with available data collected from Fortum, along with weather predictions. Collected data should also be used to evaluate the performance of the models.

3. Unit Commitment

   This subproblem consists of developing a model for solving the unit commitment problem, thereby optimizing the operation of the facilities. The optimization should be aimed at finding the schedule with the lowest possible operational costs. A definition of the unit commitment problem is provided in section 4.4.1.

4. Yearly Simulations and Sensitivity Analysis

   Use the model for unit commitment to simulate a DH system over an entire year. Then compare the results with the systems actual operation during that period in order to evaluate the model. Multiple simulations with different conditions should be performed, to do a sensitivity analysis which yields economical insight about the system. The primary target should be to evaluate a possible investment in a TES.

1.3 Limitations

Since optimization of DH production is a very comprehensive problem, some limitations has been made for the execution of this study.

Methods for meteorological predictions have not been studied. When developing models for prediction of HL, only the actual measured temperatures have been used. In reality there will also be a difference between predicted temperatures and measured temperatures. This error carries over to the predicted HL.

In order to reduce the mapping job of the production facilities and comply with demands of confidentiality, the mapping was performed in a generalized manner. Each individual boiler has not been mapped out, rather the boilers and facilities are described more generally.

The heat transport through the DH grid has not been simulated, because it is not strictly necessary for the purpose of this study. Since hourly historical HL demand is available, the optimization is focused on the heat generation. It is simply assumed that the grid is operated in such a way that the heat is transferred to the right destination, given that the heat transfer constraints of the grid are not violated.

In reality, efficiencies of the boilers will vary depending on operation. In this study there has not been done an analysis regarding the variation of efficiency depending on variables like part load, temperatures and so on. Instead, fixed efficiencies have been used. It is, however, possible to use the developed model as a framework for researching the effect of varying efficiencies on the operation.

There has also been done some simplifications regarding energy prices. Although most energy prices will vary throughout the year, not all of the variations have been included in the yearly simulation. Since accurate hourly prices are only available for electricity, other energy prices are set to be constant throughout the year.

1.4 Literature Survey

1.4.1 Heat Load Prediction

An important part of the problem is to develop predictive models that can be used to optimize DH. Models that can predict future HL in the DH network are of particular interest here. Previous models are developed by analyzing the influencing factors on the HL (Dotzauer, 2002; Magnus Dahl, 2017; Idowu et al., 2014; Ma et al., 2014). It is well known that external factors such as outdoor temperature and consumer habits play the most important role in load prediction models (Dotzauer, 2002; Magnus Dahl, 2017; Idowu et al., 2014).

Dotzauer (2002) develops a simple model for HL prediction based on the parameters outdoor temperature and hour of the week. This model is based on the assumption that contributions from the social component and outdoor temperature are independent of each other, so that the contributions can be summed up.

Magnus Dahl (2017) develops a model where the weekly average HL is predicted. It is done by using the central boundary theorem to derive a formula for the power requirement of a collection of single buildings based on the power requirement of each building. In simple terms, the theorem states that a sum of a number of random variables tends toward a normal distribution. The constants in the derived formula is determined using feasible generalized least squares, a technique which is efficient in estimating unknown parameters in a linear regression model. Profiles for variation in HL requirements throughout the day are also made.

Idowu et al. (2014) compares the performance of four different machine learning algorithms when predicting HL based on different variables. To predict HL 24 hours ahead of time, the parameters hour of day, current HL, outdoor temperature and forecasted temperature in 24 hours, gives the best results. The machine learning algorithm that provides the highest precision in predictions out of the four algorithms tested is Support Vector Regression. Mixed Linear Regression provides second best results. Both of them are regression methods that are more sophisticated than regular linear regression. The report also shows that there is a significant correlation between current HL and HL in 24 hours.

Ma et al. (2014) develops a statistical model, which is based on a Gaussian mixture model. The main finding of the article is that the factors time and building type is important for determining energy consumption patterns.

Kato et al. (2008) compares the efficiency of two different neural networks in predicting power consumption. They are a feed forward neural network (FFNN), which is one of the machine learning algorithms used by Idowu et al. (2014), and a recurrent neural network (RNN). The FFNN is less accurate for dynamic HL prediction, and it is shown that the RNN is more effective.

1.4.2 The Unit Commitment Problem

As mentioned, the problem of heat generation scheduling in a DH system is variation of the unit commitment problem. This problem is well explored in the literature (Swarup and Yamashiro, 2002; Kazarlis et al., 1996; Cohen and Sherkat, 1987; Ouyang and Shahidehpour, 1991; Thakur and Titare, 2016; Damousis et al., 2004; Dasgupta and McGregor, 1994; Sakawa et al., 2002). Most of these papers deal with the unit commitment problem in electric power systems, but mathematically this is very similar to the unit commitment problem in DH systems (Dotzauer, 2003, p. 2).

An example of a DH unit commitment problem is Sakawa et al. (2002). That problem was solved by using the genetic algorithm, in a similar way to some unit commitment problems in electrical power systems (Dasgupta and McGregor, 1994; Swarup and Yamashiro, 2002; Kazarlis et al., 1996; Damousis et al., 2004). Disadvantages of the genetic algorithms are their long execution time and that the solution is not guaranteed to be optimal (Damousis et al., 2004, p. 2).

Another prominent solution methodolgy to unit commitment problems, is dynamic programming. It is used in multiple papers (Thakur and Titare, 2016; Ouyang and Shahidehpour, 1991; Cohen and Sherkat, 1987). Critic against that method revolves around its explosion of computational resource requirements with system size (Damousis et al., 2004, p. 2). Solution methodolgies based on other optimization strategies exist as well. Examples are priority lists (Senjyu et al., 2003), mixed integer linear programming (Carrion and Arroyo, 2006) and lagrangian relaxation (Cheng et al., 2000).

The method for solving the unit commitment problem employed in this paper is based on a genetic algorithm, and is presented in detail in section 4.4.2.

Chapter 2

Assessment of the Plants

This chapter is dedicated to providing an assessment of Fortum Oslo Varme's DH system. Compared to other systems in Norway, it is relatively extensive. It consists of 11 different production facilities with a total of 43 boilers, which have a combined generation capacity of approximately 1 GW. The following energy carriers are used:

- Bio-oil/bio-diesel
- Electric boilers
- Heat pumps
- Industrial waste
- Liquefied Natural Gas (LNG)
- Municipal waste
- Oil
- Pellets/biofuel

Each boiler has specifications depending on which energy carrier it uses. The specifications are described using well known measures from unit commitment literature, namely minimum down time, minimum up time, minimum generation capacity and ramp up/down rates.

Energy carrier	Min generation capacity [MW/MW]	Ramp up rate [1/h]	Ramp down rate [1/h]	Min up time	Min down time	Min down time (from standby)	Efficiency [1]
Industrial waste	0.7667	1	1	1 h	12 h	3 h	0.88
Municipal waste	0.7667	-	-	1 h	12 h	3 h	-
Pellets	0.6429	1	1	30 min	1 h	-	0.92
Oil	0.2	1	1	10 min	15 min	-	0.95
LNG	0.2	1	1	10 min	15 min	-	0.92 - 0.95
Heat pump	0.4	1	1	10 min	15 min	-	2.8
Electricity	0.1	1	1	10 min	10 min	-	0.99

Table 2.1: Overview of boiler specifications by energy carrier

For the convenience of the reader, all of the measures are explained briefly here. Minimum down time is the time it takes for a boiler to be turned back on after it has been turned off, while minimum up time is the time it takes for a boiler to be turned off once it has become active. Minimum generation capacity is the lowest possible HL the boiler can deliver, and ramp up/down rates are the rates at which the HL of a boiler can change (while it is turned on).

In reality, the specifications of a boiler depend on the configuration and physical properties of the individual boiler, but here it is assumed that the boiler specifications can be classified by the energy carrier of the boiler only. Table 2.1 shows the resulting specifications of the boilers by energy carrier. In the table, minimum generation capacity is given relative to the maximum generation capacity. For the purpose of the optimizations presented in subsection 4.4.2, it has been assumed that boilers which can use either oil or LNG, uses the cheaper of the two, namely LNG.

Ramp up/down rates are given as the maximum change in part load per hour. Most of the boilers can reach their maximum generation capacity or be switched completely off inside one hour. Those units have both a ramp up rate and a ramp down rate equal to one. The industrial waste boiler is obviously slower at ramping up or down, but its high minimum generation capacity means that it is reasonable to assume that it can ramp from minimum generation to maximum generation in approximately one hour.

Facility number	Number of boilers	Installed capacity [MW]
1	3	42
2	3	145
3	5	150
4	6	57.5
5	1	100
6	2	25
7	2	23
8	7	243
9	3	11.6
10	7	151
11	4	59

Table 2.2: Overview of the production facilities

Since the municipal waste boilers owned by Fortum can generate free heat, they are always running at their maximum generation capacity. This is true even in the summer, when the free heat is not actually needed. For this reason there is limited information available about their specifications.

As the optimization approach presented in subsection 4.4.2 utilizes a minimum time interval of one hour, minimum up or down times of one hour or less will not affect the optimization model. Therefore, such constraints do not have to be enforced.

The layout of the district heating grid is presented in figure 2.1. Because of the confidentiality of the information, it is not a geographically accurate representation. Facility names have been replaced by numbers, and no names of places are specified. Each production facility consists of one or more boilers. Table 2.2 shows the number of boilers and installed capacity at each facility.

A generalized facility is shown in figure 2.2, and it can have multiple turn and return pipes, which lead to different parts of the grid. Valves attached to these pipes control the HL delivered, so that the demand of each area is met.

The facility shown consists of four boilers, but as mentioned that number will vary between facilities. In order to satisfy heat demands at different temperature levels, the two valves by-passing the boilers are used. By adjusting the flow of water outside the boilers, the temperature

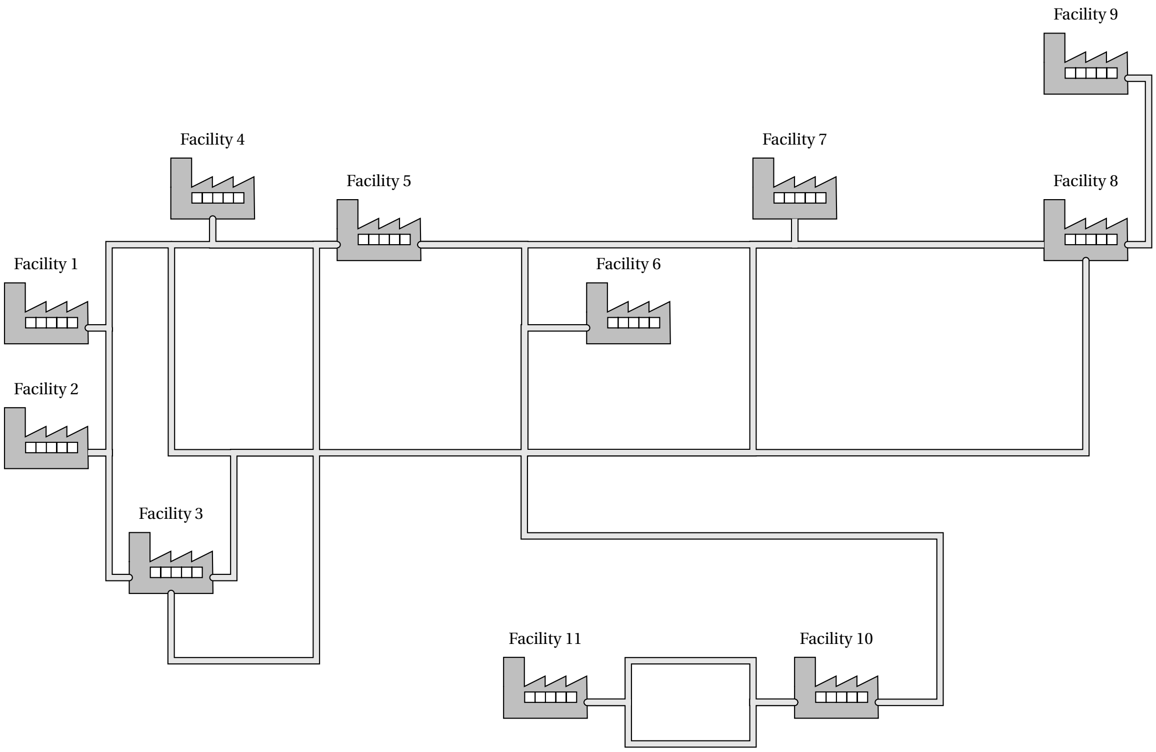

Figure 2.1: Layout of Oslo's district heating grid

level in the turn pipes can be regulated. Lower temperatures in the turn pipes, leads to lower heat losses, but it is important that the minimum temperature requirements of the customers are always met. In this case, the facility has three pumps placed in parallel. Utilizing multiple pumps, ensures reliability in case of a breakdown of one of the pumps.

A generalized overview of a boiler is presented in figure 2.3. At the primary side, the boiler is connected to a pump and valves which control the flow of water into the primary side of the heat exchanger. Increasing the flow over the heat exchanger leads to increased heat transfer to the secondary side. There is also a valve bypassing the heat exchanger on the primary side. Adjusting the flow of water to through that valve, makes it possible to control the temperature of the return water into the boiler.

There is also a feed water tank connected to the return water on the primary side. Its purpose is to feed more water into the system if the water pressure becomes too low. The valve on the secondary side controls the flow over the heat exchanger on that side. If a boiler is switched off, that valve can be closed, so that the water will flow to the other boilers instead.

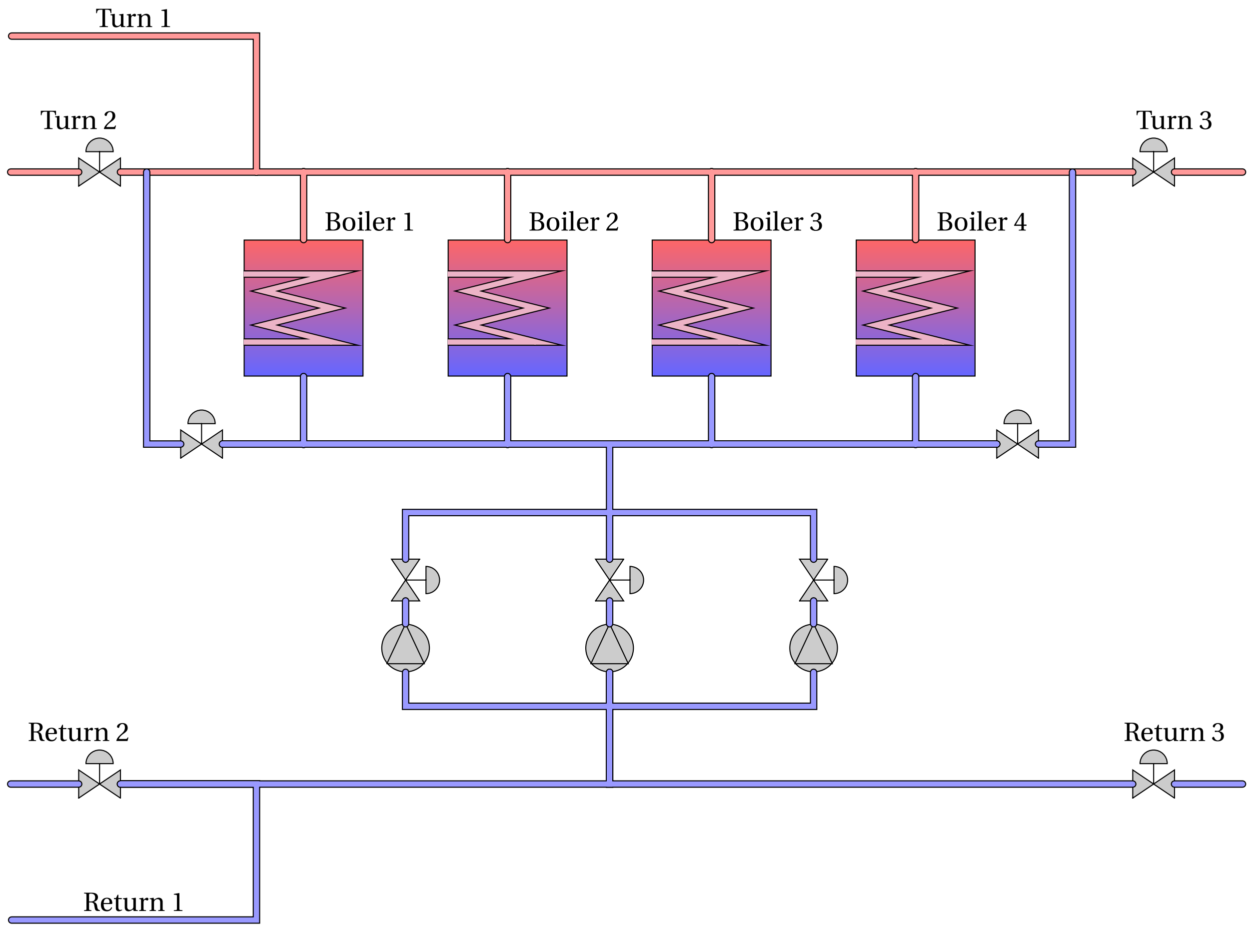

Figure 2.2: General layout of a facility

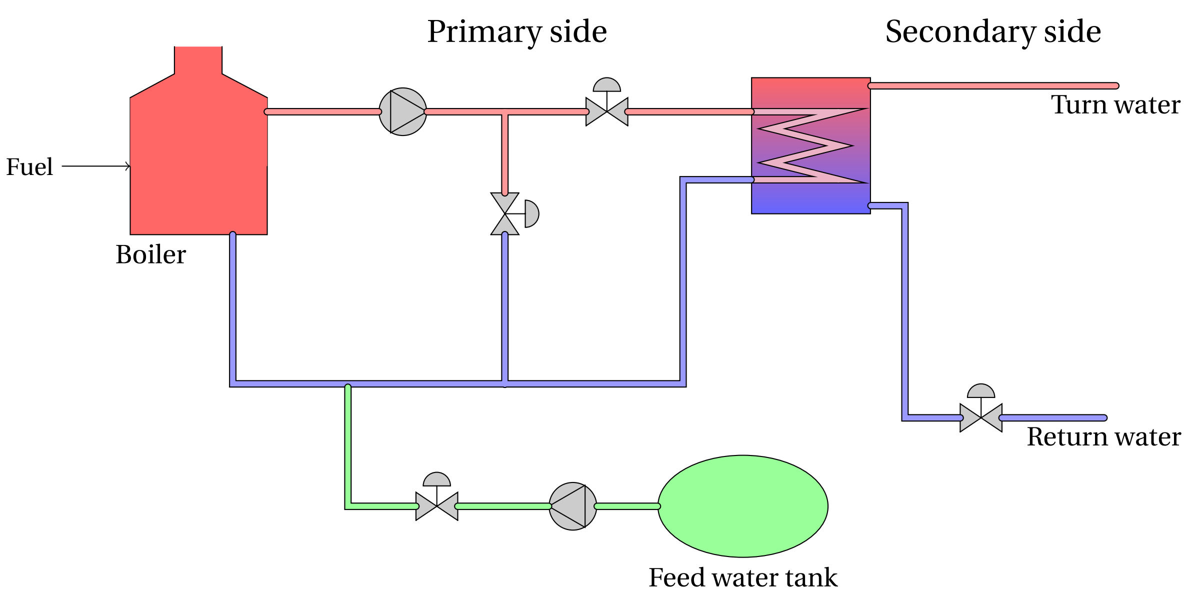

Figure 2.3: General layout of a boiler

2.1 Limitations of The District Heating Grid

As the facilities are geographically spread throughout the DH grid, the heat transfer limitations of the grid affect the operation of the facilities. The mass flow rate, $\dot{m}$, will be the limiting factor along with the temperature difference of the system, $(T_{turn} - T_{return})$. They limit the energy flow $\dot{E}$, as described by equation 2.1. When both are at their maximum values, the result is the maximum energy flow. The mass flow is in turn restricted by the diameter and roughness of the pipe, and the pumps used to pump the water through the pipe. c_v is the heat capacity of water at constant volume.

$$\dot{E} = \dot{m} \cdot (T_{turn} - T_{return}) \cdot c_v \tag{2.1}$$

Boilers which deliver heat to certain areas of the grid have upper limits on their combined generation, due to the limitation on the energy flow. Generally, this can be described by equation 2.2. Here, J is the set of units which are affected by a certain constraint. $\dot{E}_{max,J}$ is the maximum combined generation limit and, $P_j(t)$ is the generation of unit j at time t. In general, there can be many constraints on this form, but for this system there are only two such constraints which are relevant.

$$\sum_{j \in J} P_j(t) \leq \dot{E}_{max,J} \tag{2.2}$$

2.2 Operational costs

The operational costs consist of start costs, standby costs and specific energy costs. Start costs are the cost of heating the boilers to operational temperature. Standby costs are related to keeping boilers warm and ready to start generating with a lesser delay. Specific energy costs are simply the fuel costs per MW of heat at normal operation. In reality, there is also operational costs associated with maintenance and wages, but these costs are assumed to be independent of plant operation. Based on that assumption, those expenses can be neglected by the optimization model.

The boilers have start costs corresponding to the amount of energy which is needed to reach a high enough temperature to start delivering heat to the grid. Boilers powered by pellets, municipal waste or industrial waste will need start up energy in the form of bio-diesel or oil. The rest of the boilers simply use their primary energy carrier as start up energy. The start costs are calculated according to equation 2.3. The notation for the equation is given in table 2.3.

$$SU_i = \frac{P_{i,min} \cdot T_i^{off} \cdot SF_i}{2} \tag{2.3}$$

SU_i	start up cost of unit i
$P_{i,min}$	minimum generation capacity of unit i
T_i^{off}	minimum down time of unit i
SF_i	start fuel cost of unit i

Table 2.3: Notation for equation 2.3

Boilers running on industrial waste have the additional option to be in standby mode. This means that the boilers are kept warm by combustion of bio-diesel, so that generation can resume when needed. This significantly decreases the minimum down time of those units, but comes at the cost of the bio-diesel which is used to keep it warm. As suggested by equation 2.3, a shorter minimum down time will also decrease the start cost. Therefore, it may be cheaper to keep a unit at standby than to turn it off completely depending on the scheduled down time. Start costs, standby costs and specific energy prices are given in table 2.4.

Some of the municipal waste boilers in the system are not owned by Fortum. Those boilers are operated by an external company, and Fortum has simply agreed to buy all the heat they deliver at fixed rates. During the period May-September the rate is 100 NOK/MWh and during October-April the rate is 270 NOK/MWh.

Energy carrier	Specific energy price [NOK/MWh]	Standby cost [NOK/MW]
pellets	380	-
oil	720	-
LNG	390	-
heat pump	spot price + 60	-
electricity	spot price + 60	-
industrial waste	32	112
municipal waste	0	112
municipal waste (external)	100 or 270	-

Table 2.4: Operating costs of boilers by energy carrier

Electricity is traded on an hourly basis at the Nord pool power market, and the spot price is volatile over the course of a day. To accommodate for variations throughout the days, hourly price data has to be collected. Hourly spot prices has been gathered from (Nord Pool, b). It is assumed that the energy price payed by Fortum is the Nord Pool spot price plus a premium of 60 NOK/MWh.

The remaining energy prices do not vary significantly over the course of a single day, so they are assumed to be constant over time. That price data was gathered from Fortums internal data systems. In those prices, efficiency of the boilers are already accounted for. The specific energy prices for electric boilers and heat pumps, on the other hand, do not account for efficiencies. All the energy prices are presented in table 2.4 along with standby costs. The standby cost is given relative to the maximum generation capacity of the boiler.

2.3 Thermal Energy Storage

TES refers to a system which stores heat in some medium over longer or shorter periods of time. The energy can be stored as sensible heat, latent heat or thermochemical energy (Sharma et al., 2009, p. 4-5). In the context of this thesis, the term refers to systems using water to store energy as sensible heat, also called accumulator tanks.

The principle of a water based TES, is to keep hot and cold water separated inside the tank. No built-in physical boundaries are necessary for this purpose. Instead, the difference in density

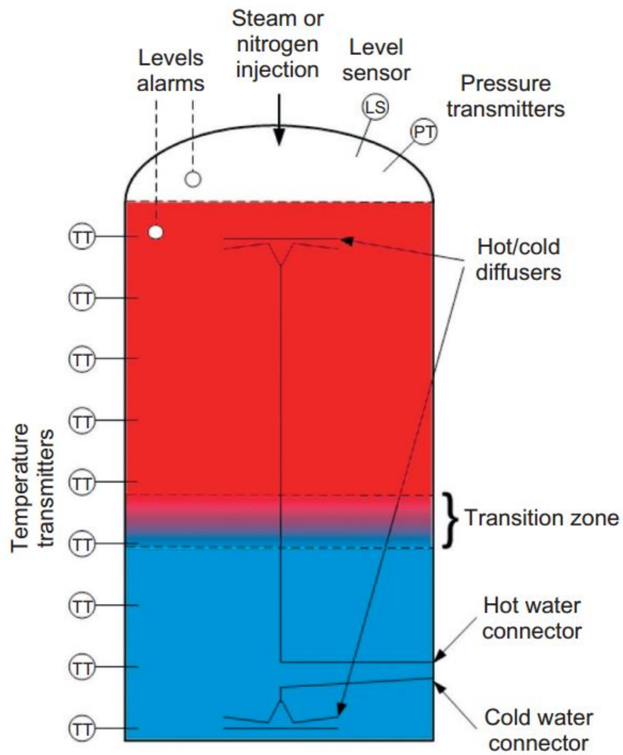

Figure 2.4: Layout of a thermal energy storage from Thomsen and Overbye (2016)

between hot and cold water ensures that the hot and cold water stays separated in layers. Hot water with low density will stay in a layer on the top part of the tank, while cold water with higher density will stay lower down. In the middle there is a transition zone with a temperature gradient ranging from hot at the top to cold at the bottom. This phenomenon is called stratification (Thomsen and Overbye, 2016, p. 3-4).

The tank is always completely filled with water, but the ratio between cold and hot water changes as heat is charged or discharged. When the storage is in discharge mode, hot water is extracted from the top, and cold water is fed into the bottom. In charge mode, hot water is fed in at the top, and cold water is extracted at the bottom (Thomsen and Overbye, 2016, p. 3-4).

Since the tank is designed without any physical separation of hot and cold water, it is important that the turbulence of the flows in and out of the tank is kept a minimum. To minimize the turbulence, diffusers are used to feed and withdraw water from the tank (Thomsen and Overbye, 2016, p. 3-4).

2.3.1 Operational Losses

A thermal energy storage will have two sources of operational losses. One of them is the heat losses from the tank to its surroundings caused by conduction through its walls. Heat is transferred from the water inside the tank to the colder air outside (Bahnfleth and Musser, 1998, p. 3).

The other phenomenon causing losses is mixing of hot and cold water in the tank. Even if a TES is designed to promote water stratification, there will still be some heat transfer between the higher and lower layers of water. In district heating, the equipment of the customers are designed to operate inside certain temperature ranges, and this places a minimum threshold on the turn temperature. Mixing of hot and cold water in the tank will leave some of the stored energy at a temperature which is lower than the minimum threshold. If the storage is not physically close to a production facility, so that the water can be reheated, this energy can not be delivered to the customers (Verda and Colella, 2011, p. 6).

The discharge efficiency ratio, ϵ, of the storage is defined in equation 2.4. Q_{av} is the average usable discharge energy of the storage, and Q_{tot} is the total initial energy (Verda and Colella, 2011, p. 6). It will vary depending on the design of the tank, and the charging/discharging rates. Higher flow rates will make the flow more turbulent, increasing the losses due to mixing (Verda and Colella, 2011, p. 6). The insulation of the tank affects the losses due to conduction.

$$\epsilon = \frac{Q_{av}}{Q_{tot}} \tag{2.4}$$

Verda and Colella analyzes a tank with a volume of 1000 m^3. Using a one dimensional model and computational fluid dynamics, a discharge efficiency ratio of between 90% and 86% depending on discharge rate is found. This is also consistent with values in other works (Bahnfleth and Musser, 1998, p. 3) (Wang et al., 2015, p. 7). For the purpose of the optimization model, a value of 90% has been chosen.

2.3.2 Dimensioning

The storage capacity, $E_{TES,\max}$, is determined by the internal volume of the tank, V, and the temperature difference of the water, $(T_{turn} - T_{return})$. It is calculated according to equation 2.5.

$$E_{TES,max} = V \cdot \rho \cdot c_p \cdot (T_{turn} - T_{return}) \tag{2.5}$$

c_p is the heat capacity of water, and ρ is the density of the water. The charge/discharge capacity, $P_{TES,\max}$, is not that clearly defined. When the charge/discharge rate is increased, the flow becomes more turbulent. This, in turn, increases the mixing of hot and cold water, and thereby reduces the discharge efficiency ratio. For this reason, the charge/discharge capacity must be set based on the desired discharge efficiency ratio.

Chapter 3

Presentation of Data

The purpose of this chapter is to give an overview of the DH system at hand. This is done by studying operation of the system over time and reviewing relevant historical data. Both internal and external parameters have been reviewed.

3.1 Outdoor Temperature and Heat Load Data

Some of the outdoor temperature data and HL data used to create the models for HL prediction in chapter 4 are presented here. The dataset consists of hourly averages from the period 2013 - 2016. Only data from 01-Jan-2016 01:00:00 - 31-Dec-2016 08:00:00 is presented here. Outdoor temperatures are recorded at Ullevål. HL is the total heat delivered from all boilers across all eleven plants. In other words, it is the total heat that is delivered to Oslo's DH grid.

As figure 3.1 and figure 3.2 suggests, the data tends to follow a trend where the relationship between HL and outdoor temperature are approximately linear below a threshold temperature, $T_{threshold}$. When the outdoor temperature is higher than $T_{threshold}$, HL is approximately constant at the value P_0. This relationship can be explained by the fact that there is no need for room heating when the outdoor temperature is over $T_{threshold}$. In that range the only source of HL demand is from tap water heating (Magnus Dahl, 2017; Dotzauer, 2002).

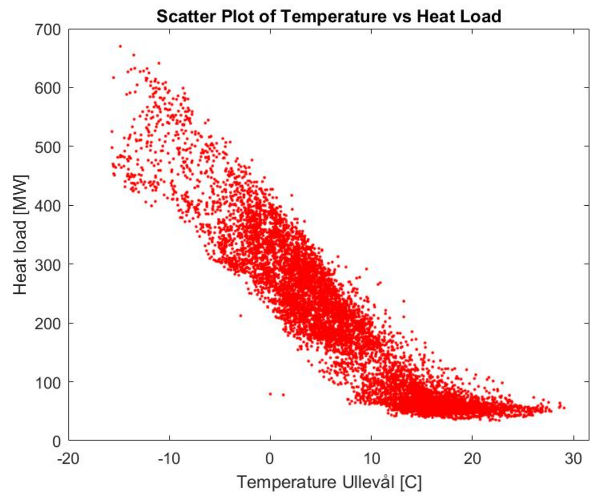

Figure 3.1: Scatter plot of hourly heat load versus temperature Jan-2016 01:00:00 - 31-Dec-2016 08:00:00

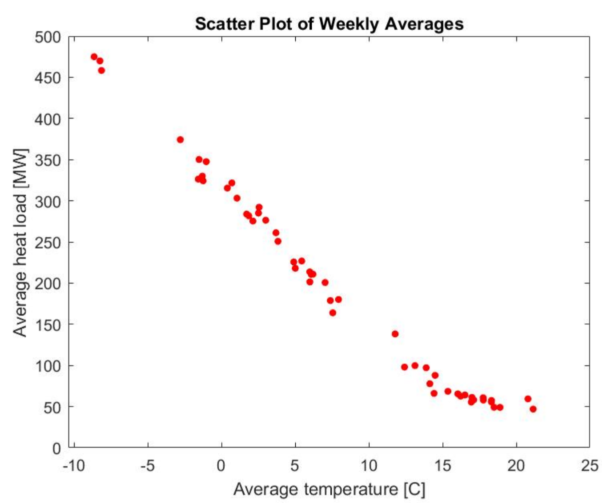

Figure 3.2: Scatter plot of weekly average heat load versus weekly average temperature Jan-2016 01:00:00 - 31-Dec-2016 08:00:00

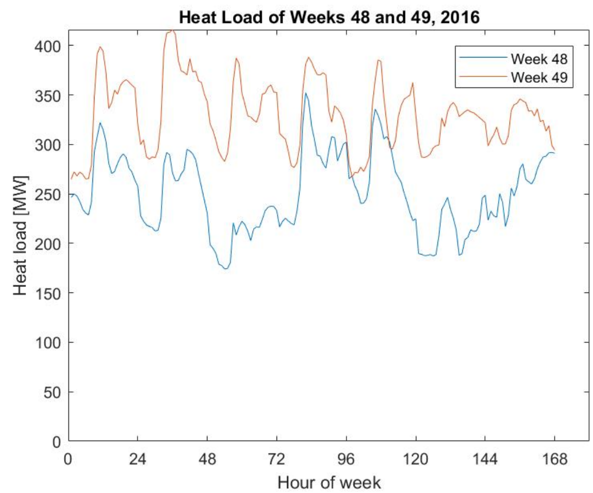

Figure 3.3: Hourly heat load of weeks 48 and 49, 2016

Notice that the data points are more scattered in figure 3.1 than in figure 3.2. The reason for this is that hourly HL is heavily influenced by the daily consumption patterns. When taking the average over one week, the daily consumption patterns does not impact on the value. There will, of course, still be differences in consumption patterns between weeks as a consequence of for example holidays. Another reasonable contribution factor to the difference in spread is that potential outliers of the hourly data will has less impact on the weekly average data. Since each weekly data point is the average of 168 hourly data points, a couple of outliers in the hourly data will not have a big impact on the weekly average value.

Figure 3.3 shows how the HL varies depending on the hour of the week for two consecutive weeks. For weekdays, there are usually two peaks, one in the morning and one in the evening. During the night HL stays at a lower value. The high peaks induce increased costs, because they need to be covered by more expensive energy sources. This is part of the motivation for using accumulator tanks to store energy.

It is also worth noting that the daily profiles of weekends are different from those of weekdays. The reason for this is differences in consumer patterns between weekends and weekdays (Ma et al., 2014). More people get up early and go to work in the week, whereas they get up later and stay at home in the weekend. When people get up, there is an increased demand for tap water heating due to showering. Demand for room heating also increases. On work days the heat demand of work places will be higher during opening hours, while homes will have reduced demand in this period (Gross and Galiana, 1987, p. 4). These differences are important to take into consideration when developing models for HL prediction.

3.2 District Heating Operation

To be able to evaluate the model for unit commitment, it is useful to study historical operating data for comparison. It can reveal information about how the system operates as well. This section contains HL data from facility 8 along with the total HL demand of the system. The data is presented as hourly values for one day at a time. To get a good overview, one day from each season except autumn where selected. Autumn was omitted, as meters seems to have malfunctioned during that period, so that data was not available.

Figure 3.4 and figure 3.5 shows how total HL demand and HL of each individual boiler varies on 01.01.2016. As one can see, the HL demand initially is at about 240 MW and then rises to around 300 MW between 7:00 and 8:00. It then stays around 300 MW until it starts slowly decreasing after 16:00. Before midnight the HL demand is back to approximately 240 MW.

Looking at figure 3.5 it does not seem like the changes in total HL demand carries over to the HL of the boilers at facility 8. The explanation for this must be that boilers located in other facilities are ramped up to meet the increased demand. Boiler 5, which uses industrial waste, and boilers 6 and 7, which use municipal waste, are kept switched on throughout the day. Their HL is kept steadily around their maximum generation capacity. The remaining boilers, which use pellets (boiler 1), LNG (boiler 2 and boiler 3) and electricity (boiler 4) are kept switched off. This indicates close to optimal operation of the facility, as the cheapest sources of energy are the ones being used.

The total HL demand and boiler HL on 01.04.2016 is shown on figure 3.6 and figure 3.7. The HL demand has a peak of around 150 MW between 9:00 and 10:00. After 16:00 it rises up again and stabilizes around 130 MW.

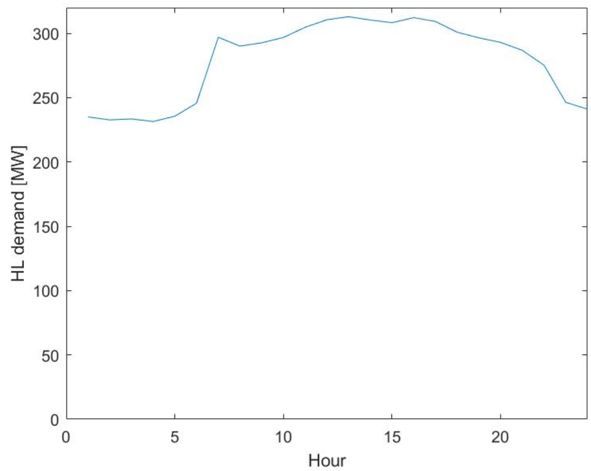

Figure 3.4: Total heat load demand 01.01.2016

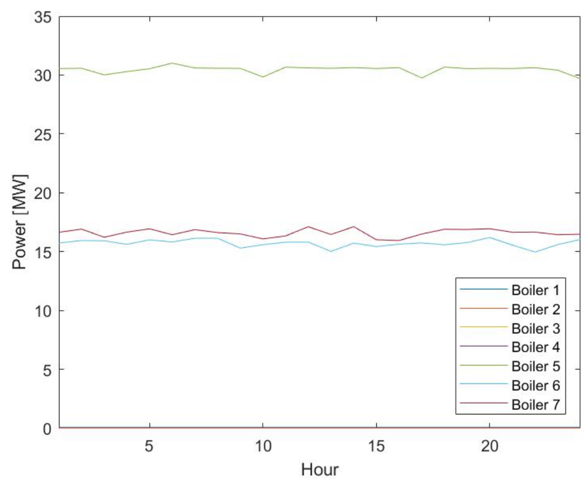

Figure 3.5: Heat load of the boilers at facility 8 on 01.01.2016

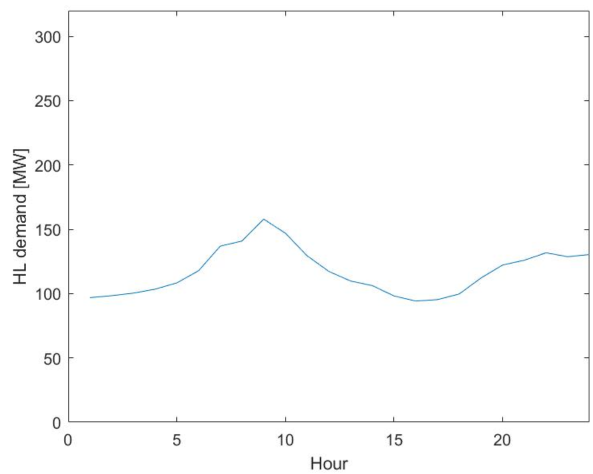

Figure 3.6: Total heat load demand 01.04.2016

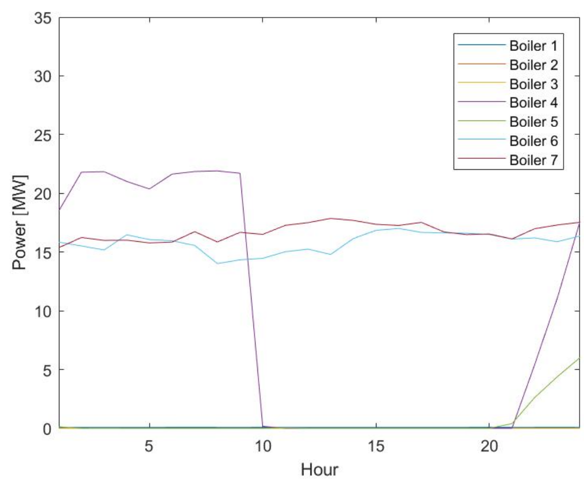

Figure 3.7: Heat load of the boilers at facility 8 01.04.2016

Once again boilers 6 and 7 are generating heat at their maximum capacity throughout the day. To meet the peak demand, the el-boiler, boiler 4, is kept on until around 10:00. After it is switched off, it remains off until after 20:00, when it is ramped back up. It might seem counterintuitive to utilize electricity rather than industrial waste to cover the peak demand. After all heat from industrial waste is far cheaper than electricity. This can, however, be explained by the higher start cost of the industrial waste boiler. It takes longer to start up, and also consumes expensive bio-oil when doing so. Since there is large fluctuations in HL demand, it can sometimes be better to utilize the el-boiler to satisfy a temporary demand.

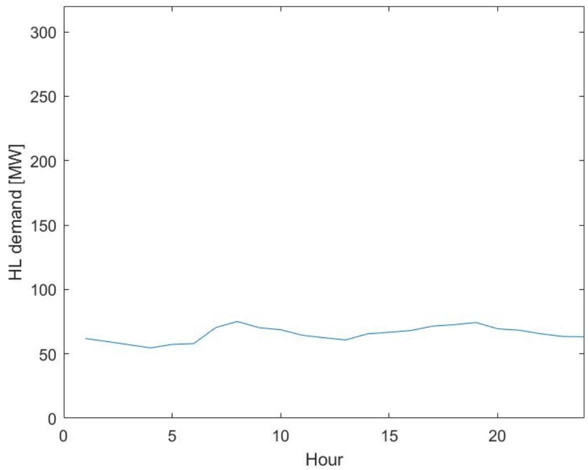

Figure 3.8: Total heat load demand 01.07.2016

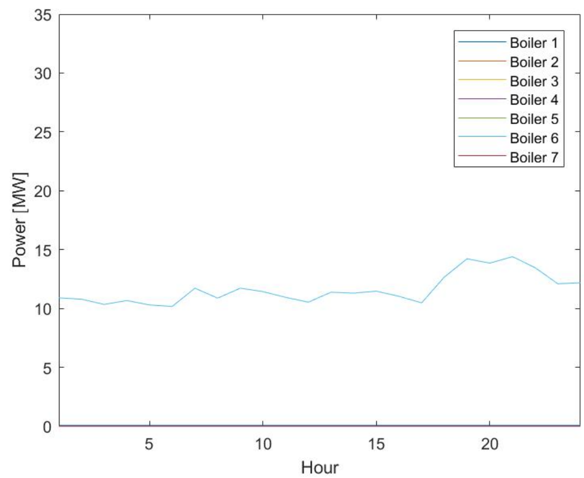

Figure 3.9: Heat load of the boilers at facility 1 01.07.2016

Finally, HL demand and boiler HL of 01.07.2016 are shown in figure 3.8 and figure 3.9. HL demand stays very low throughout the day, but with small peaks in the periods 7:00 - 8:00 and 18:00 - 19:00.

Only boiler 6 is kept on throughout the day. The reason could be that Fortum are obligated to buy the heat generated by that boiler. This is true even if heat from industrial waste would be cheaper.

Chapter 4

Methodology

This chapter is aimed at presenting the methodology which was used to solve the four tasks brought up in section 1.2. The first section contains information about how the structuring and collection of data was performed. The second section deals with a method for analyzing a known HL profile in order to decide the necessary size of a potential TES. Methodologies for predicting the HL profile based on external parameters is presented in the third section. In the fourth section, the methodology used to find the optimal operation schedule of the boilers based on a known HL profile is described.

4.1 Data Collection

The methods for collecting and structuring data are presented in this section. All of the historical data was collected from Fortums internal data systems. The collection process consists of the following three steps.

4.1.1 Retrieving Tags

The layout of the system as well as the layout of each of the facilities are represented graphically in computer program. It includes all of the important units, like pumps, boilers, regulators and so on. Each unit has an individual tag, which is essentially the name or code of that unit. To get historical values for one unit, the tag of that unit has to be retrieved.

4.1.2 Compiling a Report

Once all the necessary tags have been retrieved, the next step is to input those tags into a report creation program. The program lets one input the desired tags along with metadata like the desired time step, desired period and so on. When it runs, the output is an excel table with listings of values for each selected tag at each time step. Analyses were, for the most part, performed with one hour time steps, so that was also the selected interval for the data reports.

4.1.3 Organizing Data

To further organize and visualize the data, the excel data was later imported into matlab. In matlab's workspace one can then create variables containing any time interval and combination of tags. Most of the data were structured into separate variables for each year. For example, an individual variable containing the hourly HL demand during 2016 was created. Afterwards, separate variables were created for the HL demand of the remaining years.

4.2 Analysis of Heat Load Profile

To find out if investment in a TES is necessary, one has to perform some analysis of the HL profile of the relevant DH system. Intuitively, a system where the HL demand varies a lot during the day, will have a larger upside from using a TES. In a system with high demand peaks, a TES can be very useful in reducing said peaks. The methodology for analyzing daily HL variations is presented in the following.

To analyze the daily HL patterns, two terms introduced by Gadd and Werner are used. These are the relative daily variation, G_d, and the relative hourly variation, G_h.

4.2.1 Relative Daily Variation

The relative daily variation, G_d, is defined by equation 4.1. Here, P_h is the hourly average HL, P_d is the daily average HL, and P_a is the annual average HL (Gadd and Werner, 2013, p. 5).

The relative daily variation is a measure of how much the hourly average HL deviates from the daily average HL during a day. For one year there will be 365 different values. A TES with a size corresponding to the highest value of relative daily variation would be enough to eliminate all of the daily variations during that year. Since G_d is a unitless measure, equation 4.1 has to be multiplied by $24 \cdot P_a/100\%$ to get the storage size (Gadd and Werner, 2013, p. 5).

$$G_d = \frac{\frac{1}{2}\sum_{h=1}^{24}|P_h - P_d|}{P_a \cdot 24} \cdot 100\% \tag{4.1}$$

4.2.2 Relative Hourly Variation

The relative hourly variation, G_h, is defined by equation 4.2. It is a measure of how much the hourly average HL deviates from the daily average HL for each hour during the course of a year. A TES with a HL capacity corresponding to the highest value of relative hourly variation will be enough to eliminate all of the daily HL variations. Since G_h is a unitless measure, equation 4.2 has to be multiplied by $P_a/100\%$ to get the HL capacity (Gadd and Werner, 2013, p. 5).

$$G_h = \frac{|P_h - P_d|}{P_a} \cdot 100\% \tag{4.2}$$

4.2.3 Dimensioning of Thermal Energy Storage

The maximum values of the preceding terms specify the size and the HL capacity of a TES necessary to eliminate all of the daily HL variations. In reality, a TES which eliminates all of the variations will be oversized and therefore not the most profitable option (Gadd and Werner, 2013, p. 7).

To find a middle ground between the investment cost and reduction of HL variation, some further analysis has to be performed. Gadd and Werner suggests that one should first remove the extreme values, corresponding to the highest 1% of G_d and G_h. Then the average values of both parameters are calculated. Using the average values instead of the maximum values is sufficient to remove almost all of the daily HL variations (Gadd and Werner, 2013, p. 7).

4.3 Heat Load Prediction

In the following, two methods for HL prediction are presented. Common for both of them is the goal of predicting future values based on a set of known parameters. Both models were fitted based on data from 2015 to 2016. They were then used for predictions on data from 2013 to 2014. When training the neural network, 70% of the data from 2015 to 2016 were used for training, 15% for validation and 15% for initial testing. Both methods have been implemented in MATLAB R2017b.

4.3.1 Multiple Linear Regression

Multiple Linear Regression (MLR) is a method built on the assumption that the relationship between the dependent variable and the input parameters can be described by equation 4.3 (Idowu et al., 2014, p. 3).

$$Y = \alpha + \beta_1 \cdot X_1 + \beta_2 \cdot X_2 + ... + \beta_n \cdot X_n \tag{4.3}$$

Y is the dependent variable, $x_1, x_2, ..., x_n$ are the input parameters, and $\beta_1, \beta_2, ...\beta_n$ are the weights which describe the dependency of Y on each input parameter. There will be an error, ϵ, between the predicted value, Y, and the real value, y.

By using this model, one assumes that the dependency of HL on each of the input parameters is in fact a linear one, but in reality relationships can have any functional form. To account for this, it is possible to include input parameters which are functions of independent parameters. In this model, some of the input parameters are products of independent parameters.

In MATLAB R2017b, the method is implemented using the function *fitlm*. The model was fitted using the option of robust fitting, which is a modification of the least squares method. It iteratively reduces the effect of outliers using weighted least squares, where lesser weights are given to data points far from the initially fitted line (MathWorks, a). Since no data preprocessing to reduce outliers was performed, robust fitting is preferred over ordinary least squares.

The input parameters, $x_1, x_2, ..., x_n$, for the multiple linear regression model are as following.

- Outdoor temperature (Recorded at Ullevål)
- The HL recorded 24 hours prior to the prediction
- The month of the year (as 12 categorical variables)
- The hour of the week (as 168 categorical variables)
- The hour of the week multiplied by outdoor temperature
- The month of the year multiplied by outdoor temperature

It is well documented that HL recorded at one point in time has a correlation with HL recorded 24 hours later (Idowu et al., 2014, p. 4). This is also confirmed by including the current recorded HL as an input in the model for predicting HL in 24 hours. HL 24 hours ago then returns a p-value of 0 in the linear model created, which means that there is a 0% that they are not correlated.

Seasonal changes such as the number of daylight hours and changes in temperature, affects the behavior of consumers (Gross and Galiana, 1987, p. 4). To account for the varying consumption patterns over the year, the input variable *month of year* has been included.

HL also varies depending on the hour of the day and the day of the week (Dotzauer, 2002; Ma et al., 2014; Magnus Dahl, 2017; Kato et al., 2008). Both of these variations are captured by dividing the week into 168 hours, creating 168 corresponding categorical variables. A categorical variable is 1 if a data point is recorded at the corresponding weekly hour, and it is 0 otherwise.

Nonlinear Regression

The relationship between HL of a DH system and outdoor temperature is not linear over the entire range of outdoor temperatures (Magnus Dahl, 2017, p. 7). Rather HL as a function of outdoor temperature is approximately linear below some threshold temperature, T_0, and it is approximately constant above that temperature (Magnus Dahl, 2017, p. 18). This knowledge is possible to exploit when performing linear regression.

One way to find the threshold temperature, T_0, is to fit the parameters of equation 4.4 using nonlinear regression. It is an equation derived to the describe the dependency of weekly average HL, P^{tot}, on weekly average outdoor temperature, T_{out} (Magnus Dahl, 2017, p. 18). The data used for fitting is T_{out} and P^{tot}. The model is fitted by estimating values of the parameters a, T_0, σ and P_0. Estimation is done in MATLAB R2017b by employing the function *nlinfit*. It uses an iterative generalized least squares algorithm to fit the nonlinear regression model (MathWorks, c).

$$P^{tot}(T_{out}) = a\left[(T_{out}-T_0)\frac{1}{2}\operatorname{erfc}\left(\frac{T_{out}-T_0}{\sqrt{2}\sigma}\right) - \frac{\sigma}{\sqrt{2\pi}}\exp\left(-\frac{(T_{out}-T_0)^2}{2\sigma^2}\right)\right] + P_0, \tag{4.4}$$

where erfc is the error function, as defined in equation 4.5

$$\operatorname{erfc}(x) = \frac{1}{\sqrt{\pi}}\int_{-x}^{x} e^{-t^2}\,dt \tag{4.5}$$

A Combined Model

Since the dependence of HL on outdoor temperature has a different functional form above and below T_0, it is proposed to divide the training dataset into two sets. One set contains the data points with outdoor temperature lower than T_0, while the other set contains the data points where the outdoor temperature is higher than T_0. Then the two data sets are used to train two separate sets of MLR weights. Both are trained with the same selection of input parameters, but one is trained with the first set of data, while the other is trained with the second data set.

Having two separate sets of weights entails having two separate MLR models independent of each other. By combining these models, it is possible to get good predictions of HL whether the outdoor temperature is higher or lower than T_0. If a test data point has an outdoor temperature below T_0, HL is predicted by the first model, and if it is above T_0, HL is predicted by the second model. In this way, it is decided which model is used for prediction at each data point of the test data set. This means that the combined model used for prediction is in fact a combination of two separate MLR models.

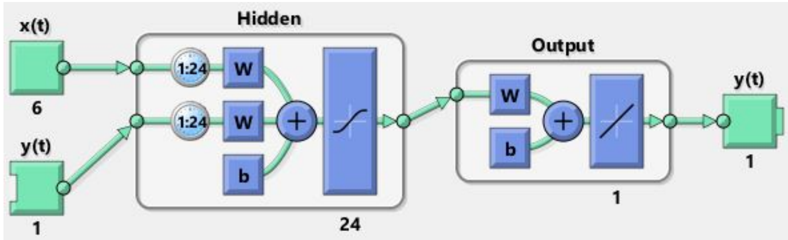

Figure 4.1: The recurrent neural network in open loop configuration (figure created in MATLAB)

4.3.2 Recurrent Neural Network

Another approach to predicting HL data, is using neural networks. In this case, a nonlinear autoregressive neural network with external input (NARX) has been used. It is a type of recurrent neural network that can learn to predict a time series given past values of the same time series, and another time series (MathWorks, b). This is shown in figure 4.1, where the watches, with 1:24 written on them, indicate delayed values.

The output of the network $y(t)$ is the HL predicted at time t. The inputs used to predict this value are $\{\mathbf{x}(t-1), \mathbf{x}(t-2), \ldots, \mathbf{x}(t-d)\}$ and past HL values $\{y(t-1), y(t-2), \ldots, y(t-d)\}$. $\mathbf{x}(t)$ is a vector of the values of K independent parameters measured at time t. In other words, for time t there are K independent input parameters $x_1(t), x_2(t), \ldots, x_K(t)$.

The independent input parameters used in this model are the following:

- The outdoor temperature
- The type of day, weekday/weekend (as a categorical variable)
- The season (as 4 categorical variables)

The output for the next time step $y(t+1)$ of the NARX network with multiple independent inputs is calculated according to equation 4.6 (Diaconescu, 2008, p. 5). The hidden layer transfer function Φ_h is the sigmoid function, and the output layer transfer function Φ_o is linear (MathWorks, d).

$$y(t+1) = \Phi_0 \left\{ b_o + \sum_{h=1}^{N} w_{h,o} \cdot \Phi_h \left(b_h + \sum_{i=0}^{d} \left[w_{i,h} \cdot y(t-i) + \sum_{k=1}^{K} w_{i,k,h} \cdot x_k(t-i) \right] \right) \right\} \tag{4.6}$$

Input x_k has a corresponding weight, $w_{i,k,h}$, for each amount of delay, i, and each hidden layer neuron, h. The output, y, also has a corresponding weight, $w_{i,h}$, for each amount of delay and hidden layer neuron. Notation for equation 4.6 is given in table 4.1.

$y(t)$	Output of the network at time step t
$x_1(t), x_2(t), \ldots, x_K(t)$	Values of K independent inputs of the network at time step t
N	Number of neurons in the hidden layer
K	Number of independent input parameters
d	Total amount of delay
b_h	Hidden layer bias
b_o	Output layer bias
$w_{i,h},\ w_{i,k,h}$	Hidden layer weights
$w_{h,o}$	Output layer weights
Φ_h	Hidden layer transfer function
Φ_o	Output layer transfer function

Table 4.1: Notation for the NARX net

The amount of delay, d, chosen for the proposed network is 24. Remember that data was collected with one hour intervals, so in time delay this corresponds 24 hours. Training of the network was done in open loop configuration using the Levenberg-Marquardt algorithm, which is described briefly by Lourakis. This means that the network was fed the correct output values, in this case HL values, when training. After the network is trained, it can be used for prediction. The future HL values are then unknown and can therefore not be used by the network. First the network has to be changed into closed loop mode as shown in figure 4.2. In closed loop mode, it uses its own predicted HL values from the previous time step as input for the next time step.

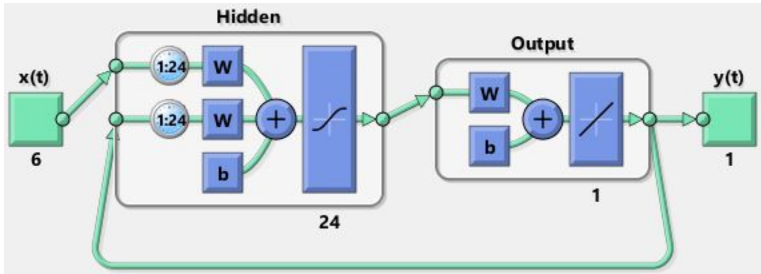

Figure 4.2: The recurrent neural network in closed loop configuration (figure created in MATLAB)

4.4 Optimization of Unit Commitment Using Genetic Algorithm and Load Dispatch

4.4.1 The Unit Commitment Problem

The short term operation scheduling of DH production is a version of the unit commitment problem. It involves deciding which units are to be committed, in other words turned on, at every point in time inside the planning horizon. This is done by minimizing the operation cost, while serving the HL demand at every hour in the interval. Additionally, constraints related to the production units has to be respected. The mathematical formulation of the problem consists of minimizing the cost function, without violating the constraints (Swarup and Yamashiro, 2002, p. 2), (Senjyu et al., 2003, p. 2), (Damousis et al., 2004, p. 2). The cost function is shown in equation 4.7, and notation is given in table 4.2.

$$CF = \sum_{t=1}^{T} \sum_{i=1}^{N} [F_i(P_i(t)) + SU_i(t) \cdot u_i(t) \cdot (1 - u_i(t-1)) + SD_i(t) \cdot (1 - u_i(t)) \cdot u_i(t-1)] \tag{4.7}$$

The unit commitment problem has a number of constraints which need to be satisfied at any given point in time:

1. System HL balance. The generation has to be equal to the HL demand.

$$D(t) = \sum_{i=1}^{N} P_i(T) \tag{4.8}$$

CF	total cost over the planning horizon
N	number of production units
T	total scheduling period
i	index of unit
t	index of hour
$u_i(t)$	commitment status (1=on, 0=off) of unit i at time t
$P_i(t)$	generation of unit i at time t
$P_{i,max}$	maximum generation capacity of unit i
$P_{i,min}$	minimum generation capacity of unit i
$L_{i,max}(t)$	maximum generation limit of unit i at time t
$L_{i,min}(t)$	minimum generation limit of unit i at time t
$D(t)$	HL demand at time t
T_i^{on}	minimum up time of unit i
T_i^{off}	minimum down time of unit i
$X_i^{on}(t)$	on time of unit i at time t
$X_i^{off}(t)$	off time of unit i at time t
$F_i(P_i(t))$	fuel cost of unit i at time t
$SU_i(t)$:	start up cost of unit i at time t
$SD_i(t)$:	shut down cost of unit i at time t
RU_i	ramp-up rate of unit i (in megawatts per hour)
RD_I	ramp-down rate of unit i (in megawatts per hour)

Table 4.2: Notation of the unit commitment problem

2. Generation limits. The generation for each unit has to be within the current generation limits of the unit. This is stated by equation 4.9.

$$L_{i,min}(t) \leq P_i(t) \leq L_{i,max}(t) \tag{4.9}$$

Notice that the generation limits for each unit are time dependent. This is because they depend on the ramp up/down constraints and the generation in the previous time step as specified by equation 4.10

$$\begin{aligned} L_{i,max}(t) &= u_i(t) \cdot \min\{P_{i,max}, P_i(t-1) + RU_i\} \\ L_{i,min}(t) &= u_i(t) \cdot \max\{P_{i,min}, P_i(t-1) - RD_i\} \end{aligned} \tag{4.10}$$

3. Unit minimum up/down time. A unit's commitment status can only be changed when equation 4.11 is satisfied.

$$\begin{aligned} T_i^{on} &\leq X_i^{on}(t) \\ T_i^{off} &\leq X_i^{off}(t) \end{aligned} \tag{4.11}$$

4. Unit initial status. Initial status of the units must be taken into account so that ramp up/down rates or minimum up/down times are not violated.

4.4.2 A Genetic Algorithm Approach

As discussed in section 1.4.2, there are multiple possible approaches to solving the unit commitment problem. The one chosen here is employing a variant of the genetic algorithm. Genetic algorithms are search techniques that can be applied to variety of problems. They are inspired by the evolution that can be observed in nature (Kazarlis et al., 1996, p. 3).

The on/off status of all the units over the planning horizon is encoded by a bit string of length $T \cdot N$ as shown in figure 4.3. One bit encodes the status corresponding to a certain unit at a certain hour. A zero in the bit string means that the unit is off, at that hour, while a one means that it is on. A bit string is also called a genotype.

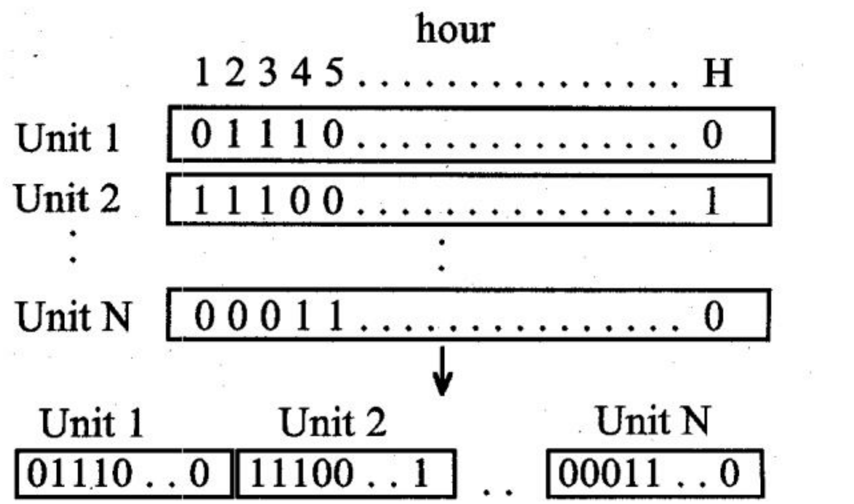

Figure 4.3: A solution to the unit commitment problem represented as a bitstring (Kazarlis et al., 1996, p. 3).

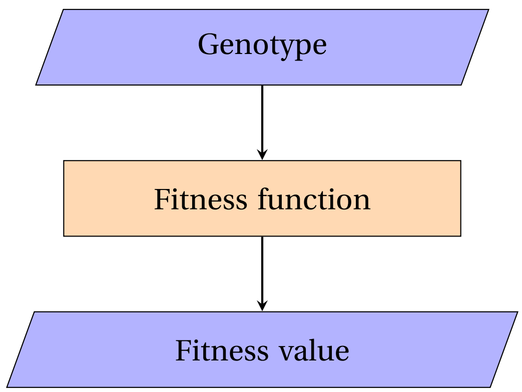

Figure 4.4: Input and output of the fitness function

Finding the optimal operation schedule is equivalent to finding the optimal genotype. The objective function which measures the performance of a genotype, is called the fitness function. It takes a genotype as input, and outputs a fitness value as shown in figure 4.4. When one is searching for the optimal genotype, one is searching for the genotype that has the lowest possible fitness value.

In the context of unit commitment the fitness value is calculated according to equation 4.12. It consists of the operation costs and a penalty term. The reason for including a penalty term is that all of the constraints of the problem are not enforced by the genetic algorithm directly. Usually some of the constraints are enforced by adding a penalty term to the cost function when the constraint is violated. This is encouraging the optimization algorithm to choose valid solutions.

The penalty is calculated according to equation 4.13 (Kazarlis et al., 1996, p. 3). In this case only the constraint of system HL balance is enforced using a penalty.

$$F_T = \left[FC_T + SU_T + SD_T + \sum_{j=1}^{N} PF_j \right] \tag{4.12}$$

FC_T:	Total fuel cost over the planning horizon with optimal load dispatch
SU_T:	Total start up cost over the planning horizon
SD_T:	Total shut down cost over the planning horizon
PF_j:	Penalty associated with violation of constraint j
j:	Constraint number

$$PF_j = \mu_j \cdot |VIOL_j|, \tag{4.13}$$

μ is the penalty multiplier associated with constraint j, and $VIOL_j$ is the amount that constraint j is being violated by.

Fitness Function

To evaluate the fitness value of a genotype according to equation 4.12, first the fuel cost and penalty has to be calculated. So in order to assign a fitness value to each genotype, the load has to be dispatched to the units at each hour to find the fuel cost. This is done by the fitness function itself. It performs load dispatch and uses the resulting fuel cost and penalty to calculate the fitness value of a selected genotype. The load is dispatched using a priority list algorithm, which minimizes the total fuel cost of each hour individually.

Before the load can be dispatched at an hour t, the current maximum generation limits, $L_{i,max}(t)$ has to be adjusted, so that the limitations of the DH grid described by equation 2.2 can not be violated. This is done by first sorting the units affected by a given constraint by descending specific energy price. Then their maximum generation limits are decreased sequentially, starting with the first unit in the list. The maximum generation limit of a unit is reduced until it either is equal to the minimum generation capacity, or until equation 4.14 is satisfied. Once it is satisfied, the combined generation limit of the affected units, $\dot{E}_{max,J}$, can no longer be exceeded, so no further changes are done to the current maximum generation limits.

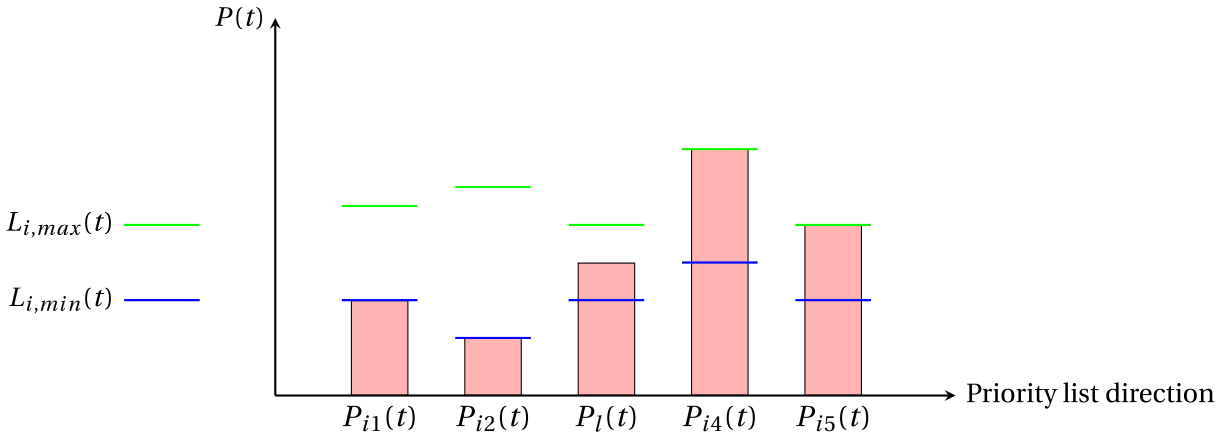

Figure 4.5: Illustration of load dispatch by priority list

$$\sum_{j \in J} L_{j,max}(t) \leq \dot{E}_{max,J} \tag{4.14}$$

When the generation limits have been adjusted, the next step is to find the optimal load dispatch at the current hour. This is in essence similar to the previous step. First a priority list is created by sorting the currently active units by descending specific energy prices. It must be prioritized to utilize the cheaper units at the back of the resulting list. This is achieved by first setting the generation of all the units to their current maximum generation limits. Then the generation of each unit is decreased sequentially, starting with the units at the front of the priority list. The generation of a unit is decreased until it is equal to the current minimum generation limit, or until equation 4.8 is satisfied. Once it is satisfied, the procedure ends.

The result will be that a sequence of units from the front of the list has their generation set to $L_{i,min}(t)$, and a sequence of units at the end has of it has their generation set to $L_{i,max}(t)$. A unit in between those two sequences will have its generation set somewhere between $L_{i,min}(t)$ and $L_{i,max}(t)$. This unit will from now on be reffered to as the limit unit or unit l. An example of a result of the load dispatch procedure is shown in figure 4.5.

Once the optimal load dispatch for an hour has been found, it is possible to calculate the fuel costs associated with that load dispatch. If the optimal load dispatch does not satisfy equation 4.8, a penalty is incurred according to equation 4.13.

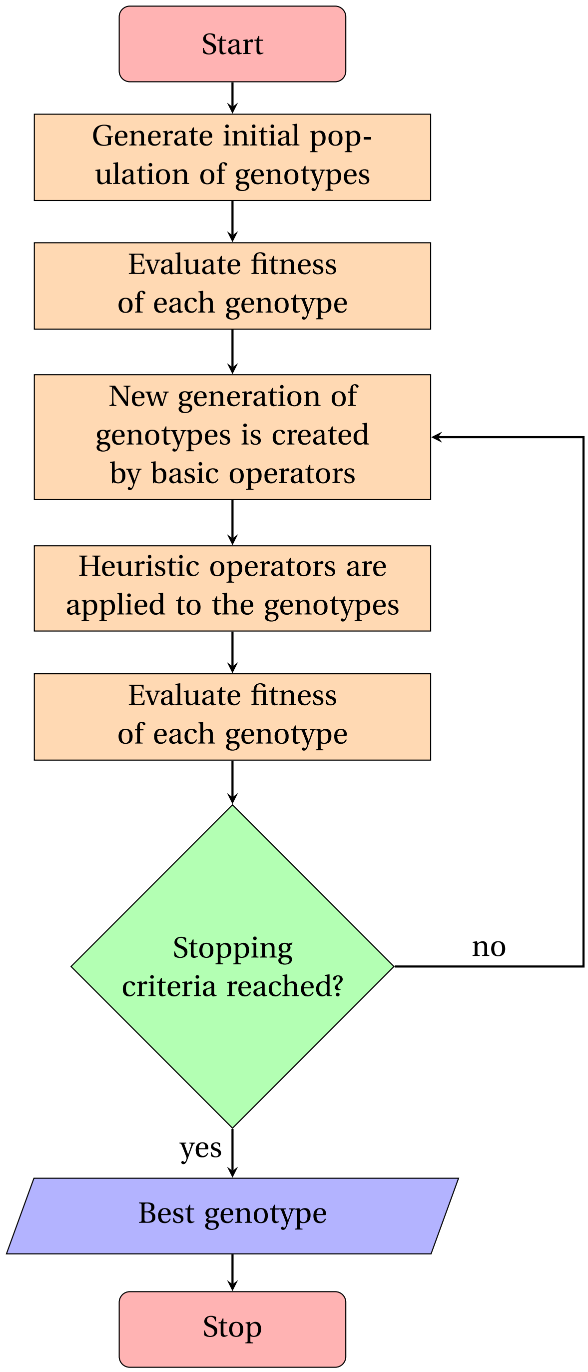

Figure 4.6: Flowchart of the genetic algorithm approach

The whole procedure is sequentially repeated for the next hours of the planning horizon. When it is finished, all of the terms on the right hand side of equation 4.12 can easily be calculated, so that the fitness value is found.

4.4.3 The Genetic Algorithm

The genetic algorithm works by randomly creating an initial set of solutions, also called a generation of genotypes. Then each genotype is evaluated by the fitness function, which assigns it a fitness value. Afterwards, it creates the next generation of genotypes from the previous one using three different operators. Before any operators are used, two parent genotypes are chosen at random, but with a larger probability assigned to genotypes with a low fitness value relative to the rest of the population. Two offspring genotypes are then created using one of the basic operators: crossover, mutation or elitism (Kazarlis et al., 1996, p. 4). This process is repeated until the desired amount of offspring genotypes have been created. The distribution of offspring creation between operators can be set at any desirable value. In the following, each basic operator is explained.

Crossover

This operator mimics the natural selection in nature. It combines the properties of the two parent genotypes, and creates a new genotype with properties from both parents. Some parts of the offspring genotype will be copied from one of the parents, while other parts of it are copies from the other parent (Kazarlis et al., 1996, p. 4).

Mutation

This operator mimics the mutation in nature, and is aimed at increasing the diversity of genotypes, in order to find better solutions. When applied, it changes randomly chosen bits of the offspring genotype from 0 to 1 or the other way around (Kazarlis et al., 1996, p. 4).

Elitism

The best individuals from the previous generation are simply copied over to the next generation without any alteration. (Kazarlis et al., 1996, p. 4).

4.4.4 Heuristic operators

The aforementioned operators are the most standard features of the genetic algorithm. They are generally effective at solving any type of problem. In this case, a number of additional operators are implemented in order to make the algorithm find better solutions specifically for the unit commitment problem. As shown in figure 4.6, once a new generation has been created by crossover, mutation and elitism, the resulting solutions are altered by a set of heuristic operators.

Turn-off mutation

A problem of using the genetic algorithm to solve the unit commitment problem, is that it is difficult for the algorithm to determine if a unit should be turned off for the entire scheduling period. The turn-off mutation is aimed at addressing this problem (Maifeld and Sheble, 1996, p. 37). It is applied to each of the solutions in a new generation with a certain probability. When it is applied to a genotpe, a unit is chosen at random, and this unit is switched off for the entire scheduling period.

Intelligent mutation I

In unit commitment, it is rarely optimal to switch a unit on and off every other hour. With this knowledge, the intelligent mutation I operator was developed. When applied to a solution, it first chooses on unit at random. Then it searches that units schedule for instances where the unit is turned on or off. In other words, it searches for 0 1 and 1 0 combinations in the schedule. When such a combination is found, it is replaced by either a 1 1 or 0 0 combination, with equal probability (Maifeld and Sheble, 1996, p. 49).

Intelligent mutation II

This operator is also aimed at finding better solutions by eliminating constant on/off-switching. Similarly to intelligent mutation I, a unit is chosen at random and searched for 0 1 and 1 0 combinations. However, instead of replacing the bits at random, the operator calls the fitness function to test whether it is cheaper to replace them by a 1 1 or 0 0 combination or leave them as is. Whichever combination gives the lowest fitness value is kept in the genotype (Maifeld and Sheble, 1996, p. 51).

Minimum Up/Down Operator

Since up and down time constraints are not enforced on the problem, a repair operator is necessary in order to fix invalid solutions. This operator searches for instances in the solution schedule where such constraints are violated. When a point is found where a unit is switched on illegally, the hours from it is turned off until the hour before it can legally be switched on are all replaced by either ones or zeros, depending on which combination gives the lowest fitness value. This is an embodiment of the Minimum Up/Down Operator (Swarup and Yamashiro, 2002, p. 4).

4.4.5 Thermal Energy Storage

Up to this point, methodology for solving the unit commitment problem with the genetic algorithm, has been presented. Similar approaches have been used to optimize the operation of DH systems to some extent (Sakawa et al., 2002, 2001). There is, however, limited information available on how the approach can be applied to DH systems which include a TES.

In this section, it will be shown that the approach can, with slight modifications, also be used for systems which have a TES. In that case, the TES is treated as a normal generator, which has its minimum and maximum generation limited by the physical properties of the storage.

Since the TES does not have a specific energy cost assigned to it, its place in the priority list of generators can not be decided with the standard priority list algorithm. To define its position in the list, a number of additional bits containing that information are needed. These are appended to the original genotype, and encode an integer, I, which defines how the storage is to be operated. For each hour of the planning horizon, k bits are added to the genotype. The integer, I, then has a value between $-k/2$ and $k/2$. Its value is calculated according to equation 4.15. Here, b_i is the value of bit i. Methods representing integers with bits from a bit string has been utilized previously in other optimization problems (Gil et al., 2003, p. 4).

$$I = -\sum_{i=1}^{k/2} b_i + \sum_{j=k/2+1}^{k} b_j \tag{4.15}$$

If the integer is negative, it indicates that the storage is charging, while a positive value indicates that energy is being discharged. A value of zero indicates that the TES is disabled.

If the value of I is -1, the storage unit will be placed immediately before the limit unit in the priority list. In case there are more units with the same specific energy price as the limit unit, the storage unit will be placed before the first of them. For each integer I is less than -1, the storage is placed one price step further to the front of the priority list.

If the value of I is 1, the storage unit will be placed immediately before the limit unit in the priority list. In case there are more units with the same specific energy price as the limit unit, the storage unit will be placed before the first of them. For each integer I is larger than 1, the storage is placed one price step further to the back of the priority list.

When the storage is in discharge mode, it has a maximum discharge capacity, $L_{TES,max}(t)$, given by equation 4.16 and a minimum discharge capacity, $L_{TES,min}(t)$, of zero. When it is in charge mode, $L_{TES,max}(t)$ is equal to zero, and $L_{TES,min}(t)$ is given by equation 4.17. Notice that the TES generates negative HL when it is in charge mode. ϵ is the discharge efficiency ratio of the TES and accounts for the losses as explained in section 2.3.1. $E_{TES}(t)$ is the currently stored energy of the TES, and $E_{TES,max}$ is the storage capacity.

$$L_{TES,max}(t) = \min\left\{\epsilon \cdot E_{TES}(t), P_{TES,max}\right\} \tag{4.16}$$

$$L_{TES,min}(t) = \max\left\{E_{TES} - E_{TES,max}(t), -P_{TES,max}\right\} \tag{4.17}$$

4.4.6 Yearly Simulation

To simulate the operation of the plant over an entire year, the previously described genetic algorithm approach is used. Unit commitment status and HL for each unit is scheduled for 24 hours at a time. The scheduling is run sequentially for each day of 2016, using HL demand data collected from Fortum. As the hourly unit commitment statuses and HL are found, the yearly production cost is obtained as the sum of the fitness values of the best solutions.

Chapter 5

Results

In this chapter, the results are presented. There are three parts. The first one contains the results of the load profile analysis. The second section contains results from the HL prediction, and the third section contains results from the yearly simulations.

5.1 Load Profile Analysis

The load profile analysis gives estimates of the size and HL capacity of the TES. The load profile of 2016 is used for the analysis. Figure 5.1 shows the relative daily variation on each day during the year when the largest 1% of the values has been removed. The mean value of relative daily variation is then 5.1%, which corresponds to a TES size of 238 MWh.

The largest value of relative daily variation is 14.9%, which corresponds to a TES size of 695 MWh. This means that a TES size of 695 MWh would be enough to eliminate all of the daily variations. However, a TES of that size would only be utilized at its maximum capacity for one day of 2016, which would not be economically ideal. Rather a TES size of 238 MWh is preferred as a starting point for the simulations which are to be carried out.

When it comes to relative hourly variation, the maximum value is 49.9%, which corresponds to a HL capacity of 91 MW. This means that a TES with a HL capacity of 91 MW would be enough to eliminate all of the hourly variations. Such a high value is not realistic in practice, since it would

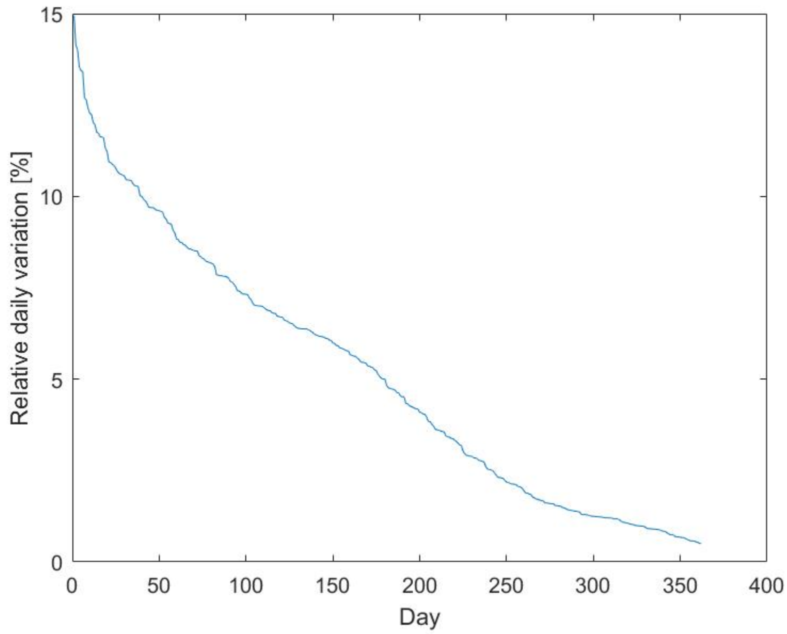

Figure 5.1: Relative daily variation for each day of 2016

require high flow rates of water. To accommodate for the higher flow rates, pipes, pump and tank has to be sized up, but even then higher water speeds relative to dimensions would likely be required as well. This, in turn, leads to more turbulence, and if there is too much turbulence the TES might be impossible to operate because of mixing of cold and hot water in the tank. The mean relative hourly variation is 10%, which corresponds to a HL capacity of 19 MW.

This analysis is useful for determining how much of the daily load variations can be eliminated with a TES of a certain size and HL capacity. However, it does not immediately show how much of the variations one should aim to eliminate from an economical standpoint. That also depends on the investment cost of the TES and the operation costs of the boilers. Therefore optimization and sensitivity analyses have to be performed in order to find the specifications of the ideal TES.

5.2 Heat Load Prediction

In this section, the results of heat load prediction using two different methods are presented. The methods used are MLR and RRN. Both models have been trained using data from 2015 to

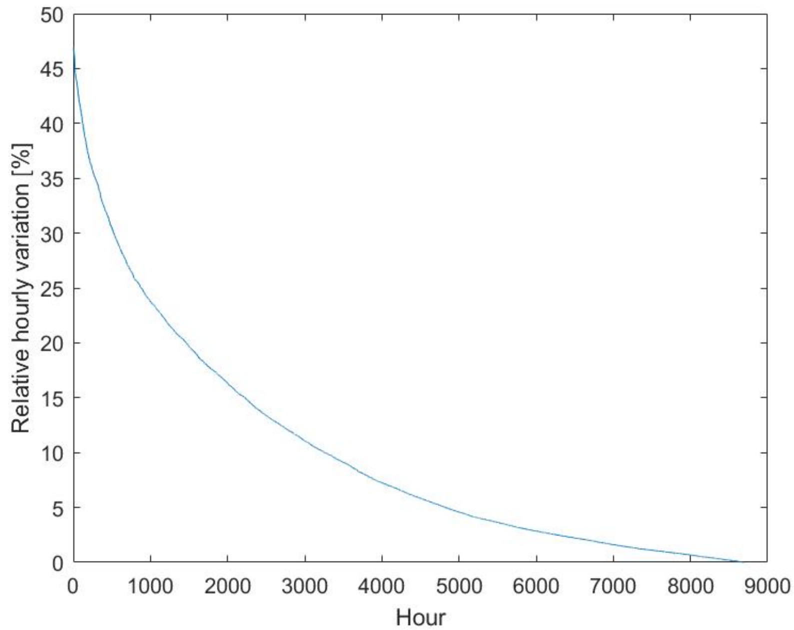

Figure 5.2: Relative hourly variation for each hour of 2016

2016, and were then tested on data from 2013 to 2014.

In table 5.1 some performance measures of the models are shown. The perfect model has Geometric Mean Bias (MG), Geometric Mean Variance (VG), Correlation Coefficient (R) and Factor of two (FAC2) equal to 1, and it has Fractional bias (FB) and Normalized Mean Square Error (NMSE) equal to 0. Both models perform on an adequate level with numbers close to the ideal values. The RNN has a lower absolute value of FB and MG, which are measures of systematic error (Chang and Hanna, 2004, p. 8). It has a better value for R as well, even if that is not necessarily indicative of a good fit (Chang and Hanna, 2004, p. 8).

The MLR model scores better on the remaining measures, NMSE, VG and FAC2. NMSE and VG are both measures of mean relative scatter. This means that the MLR makes lesser errors in its predictions overall. Its high score on FAC2 is important as well, since it indicates that almost all of the predicted values are in the vicinity of the measured values (Chang and Hanna, 2004, p. 8).

Method	Multiple linear regression	Recurrent neural network
Mean absolute percentage error (MAPE)	**7.6330**	8.7530
Fractional bias (FB)	-0.0249	**-0.0047**
Normalized mean square error (NMSE)	**0.0092**	0.0101
Correlation coefficient (R)	0.9908	**0.9932**
Factor of two (FAC2)	**0.9915**	0.9687
Geometric mean bias (MG)	0.9736	**0.9841**
Geometric mean variance (VG)	**1.0116**	1.0137

Table 5.1: Performance comparison of load prediction methods (best values in bold)

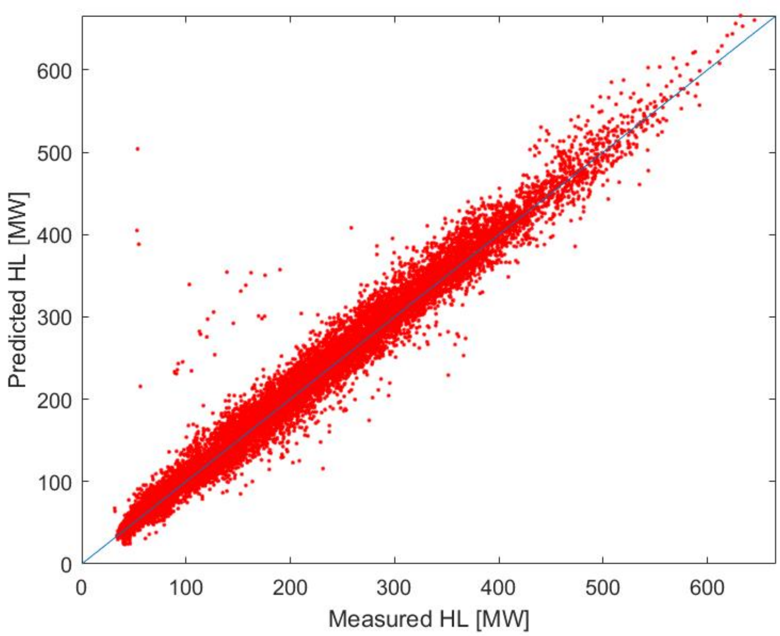

Figure 5.3: 1:1 scale plot of the multiple linear regression

Figure 5.3 shows a 1:1 scale plot of the MLR. When reviewing the plot of the MLR, some systematic errors become apparent. To the upper right of the figure, the errors do not appear to be spread randomly. Rather, all of the predicted HL are larger than the measured HL in that region. The reason for that could be an assumption made when creating the model. It was assumed that HL is linearly dependent on outdoor temperature below the threshold temperature, however, this is not completely accurate. As heating equipment is turned up to their maximum load, the HL as a function of outdoor temperature approaches a constant value (Dotzauer, 2003, p. 3).

Some large errors can be spotted in the area between measured HL of 100 MW and 200 MW. There are many points where predicted HL is more than 100 MW too high. When searching for points with an error larger than 100 MW, it becomes evident that 24 of those errors where recorded during the period 12.02.2014 - 13.02.2014. This is actually in the middle of the winter holiday in Norway, which would explain a deviation in consumer behavior from the normal consumption patterns. This uncovers a weakness in the model, namely that holidays are not accounted for.

Figure 5.4 and figure 5.5 shows the results of each sub model of the MLR model. The scatter in the upper right region of figure 5.4 suggests that a systematic error is present in the sub model for outdoor temperatures above T_0. In that region, predictions seems to systematically undershoot the measured HL. This could be caused by the observed nonlinear dependence of HL on outdoor temperature when outdoor temperature is close to the threshold temperature. As HL can not be accurately be predicted by a linear model in that area, the predictions undershoot the measured values, and also leads to some heteroskedasticity in the results.

When reviewing the scatter plot for the RNN on figure 5.6, it is evident that the predictions are more scattered away from the line. This is in line with the values of NMSE and VG presented earlier. Noticeably, both models has some extreme errors around the measured HL of 50 MW. In particular, there are three points where the predicted HL overshoots the measured HL by over 300 MW. Interestingly, all of those errors where recorded between 12:00 and 13:00 of days in august 2013. Reviewing those data points, show that the recorded outdoor temperatures are below -20 °C at each of those points, which must certainly have happened because of malfunctioning

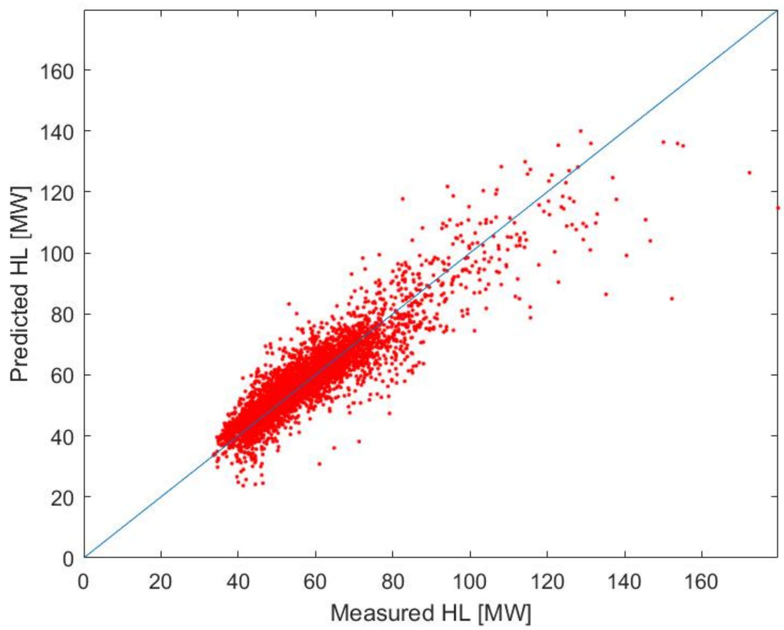

Figure 5.4: 1:1 scale plot of the multiple linear regression above T_0

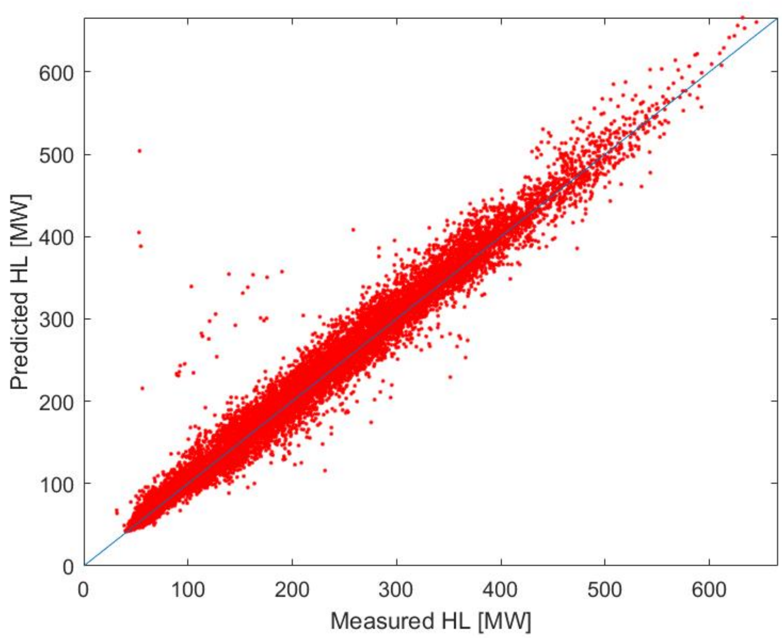

Figure 5.5: 1:1 scale plot of the multiple linear regression below T_0

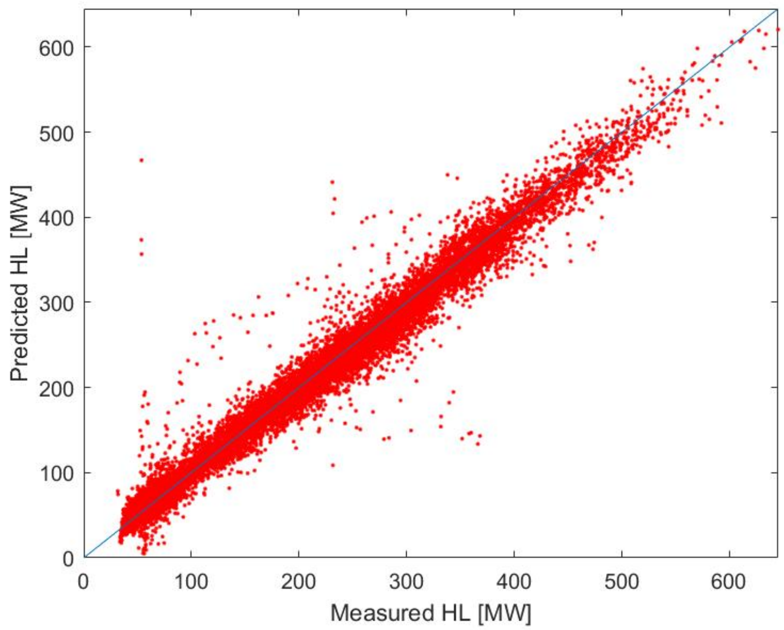

Figure 5.6: 1:1 scale plot of the recurrent neural network

measurement equipment. An interesting difference between the models is that while the MLR model overshoots its predictions in the upper right, the RNN model does not. This is related to one of the strengths of a RNN model has compared to a MLR model. To train the RNN, one does not need to make assumptions about the functional relationship between the dependent variable and the input parameters.

The prediction of both methods and the measured HL of week 2 of 2013 are shown in figure 5.7. Again it is confirmed that the linear model has lesser errors in predictions compared to the neural network. This is can possibly be attributed to the fact that it uses a larger number of parameters which affect the measured HL. Additionally, the RNN's use of previously predicted values in future predicted values can contribute to propagation of errors if initial predictions are not accurate.

The predictions and measured HL of week 30 of 2013 are shown in figure 5.8. Errors may seem larger here than in week 2, but this is because the relative errors are larger. Remember that the errors of neither model showed any clear heteroskedasticity in the 1:1 scale plots, except for a small number of data points on figure 5.4. This means that the expected magnitude of the errors

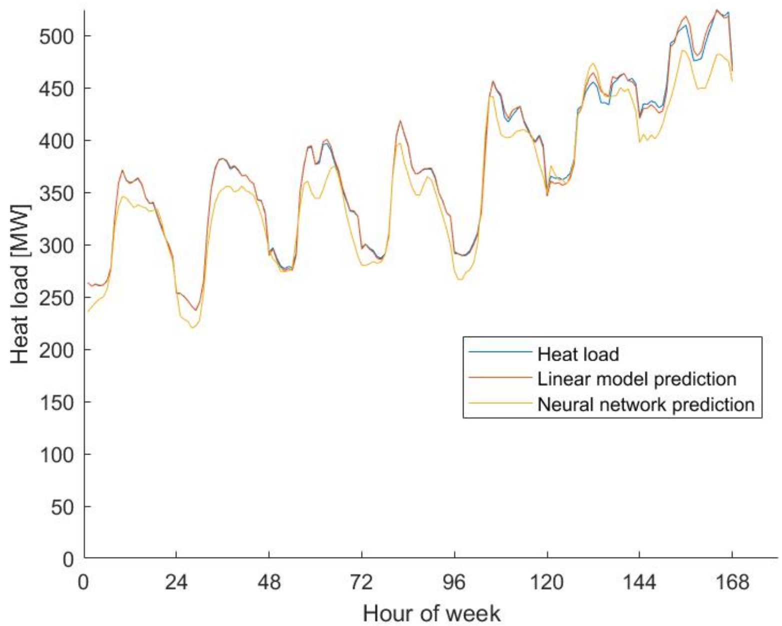

Figure 5.7: Heat load predictions of week 2, 2013

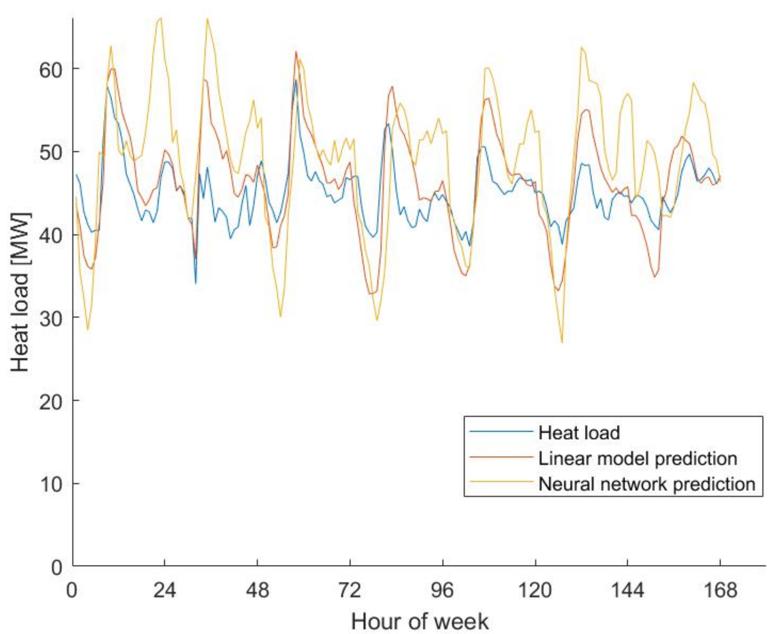

Figure 5.8: Heat load predictions of week 30, 2013

a	T_0	σ	P_0
-18.0763	14.8904	3.6738	48.5543

Table 5.2: Parameter values of non linear fitting

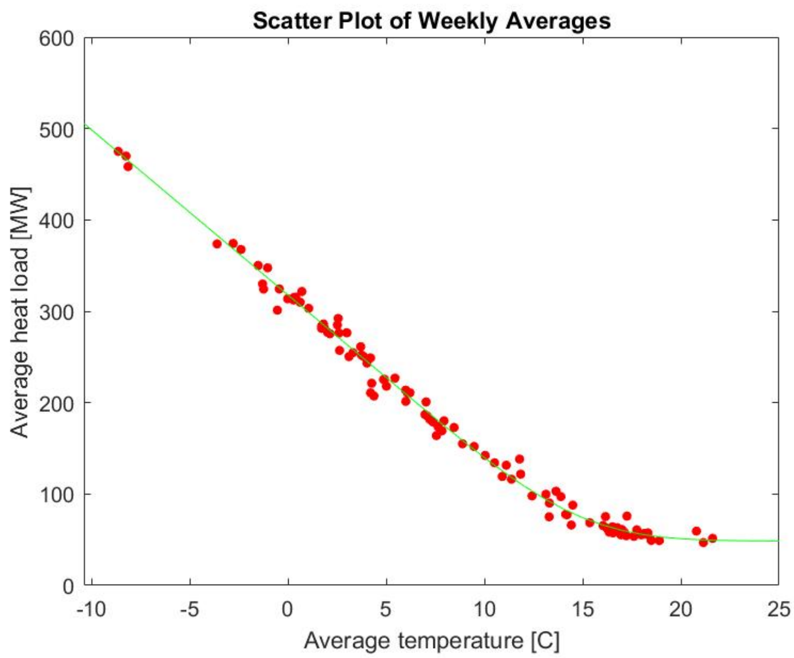

Figure 5.9: Fitted curve of non linear model to observed heat load points 2015 - 2016

is for the most part not dependent on the measured HL.

Overall, the RNN model shows less systematic bias compared to the MLR model. This is likely due to the assumption that HL is a piecewise linear function of outdoor temperature, which that model is based on. However, it does have significantly less scatter, which makes it perform better than the RNN model overall.

5.2.1 Nonlinear Regression

Figure 5.9 shows the resulting curve of the non linear regression. HL and outdoor temperature of 2015 - 2016 was used for fitting the model. The resulting values of the parameters are shown in table 5.2. Only the value of T_0 was necessary to make the MLR model.

	With TES	Without TES
Yearly cost [NOK]	184,900,000	186,240,000

Table 5.3: Results of simulations with and without a thermal energy storage

5.3 Yearly Simulation

In this section, the results of the yearly simulations are presented. Optimizations were run with a range of different setups, so that effects of various parameters can be studied.

The initial runs were carried out first without a TES, and then with a TES of size 238 MWh. The results of those simulations are shown in table 5.3. According to the results, a saving of 1,345,000 is possible with a TES of that size. Given the assumption that cost savings would be similar in subsequent years, it is possible to calculate the net present value of an investment in a TES. If one makes the conservative assumption that the lifespan of the TES is 25 years, and has an initial investment cost of 39,000,000 NOK, the net present value of the investment is -19,000,000 NOK, given an interest rate of 5% . Here, costs as a result of maintenance, tank operation, and so on have been neglected. The negative net present value indicates that the investment would not be profitable under the given conditions.

5.3.1 Comparison with Actual Operation

It is interesting to see whether the boilers at facility 8 would be operated any differently if the genetic algorithm approach was applied. In the following, the results of the yearly simulation will be presented and compared with the actual operation during that period.

On figure 5.10, the results of simulations of 01.01.2016 is presented. Operation of the industrial waste boiler, boiler 5, is similar to the operation data from figure 3.5. The HL of Boiler 6 and boiler 7 is the equal to the operation HL, as those boilers are not part of the optimizations. Boiler 4, the electric boiler, is the only one with clear differences between actual operation and simulations. The simulation has it active between hour 6 and 24, while operation data shows that it was inactive in that period. However, the difference does not make a big impact on the operation cost, as it is possible that heat from boiler 4 simply replaces the heat that would otherwise

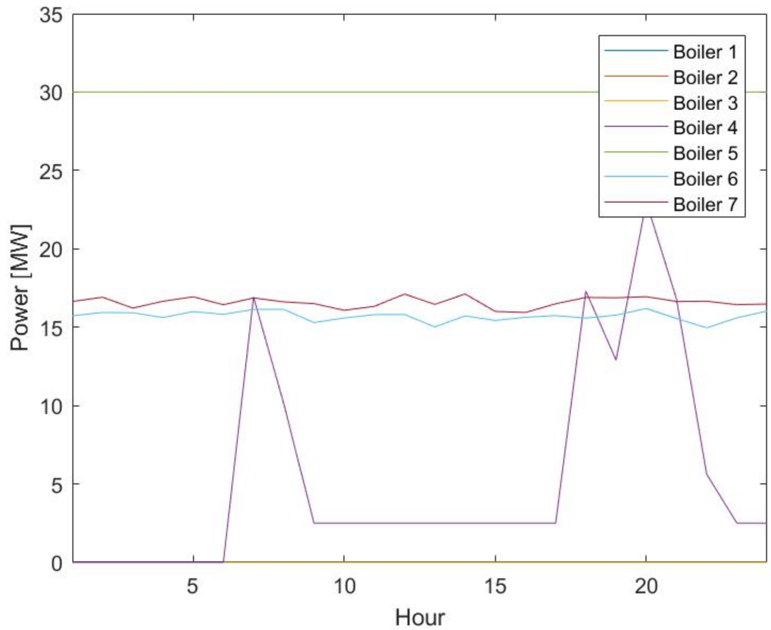

Figure 5.10: Heat load of the boilers at facility 8 on 01.01.2016

be generated from an electric boiler in another facility.

Figure 5.11 shows the results of simulations of 01.04.2016. Compared to the actual operation from figure 3.7, the major difference here is that boiler 5 is turned on instead of boiler 4. This is the cheaper solution, since industrial waste has a lower specific energy price than electricity. Seemingly, the genetic algorithm has found a more optimal operation schedule than the one used in practice. There could, however, be natural reasons for why boiler 5 is not utilized. For example there could be carried out maintenance on that boiler.

Results from optimization of 01.07.2016 are shown on figure 5.12. Here the actual operation from figure 3.9 is equal to that resulting from optimizations. The reason is that the solution is trivial. The demand is so low that no HL is generated except that from boiler 6, which is not operated by Fortum Oslo Varme.

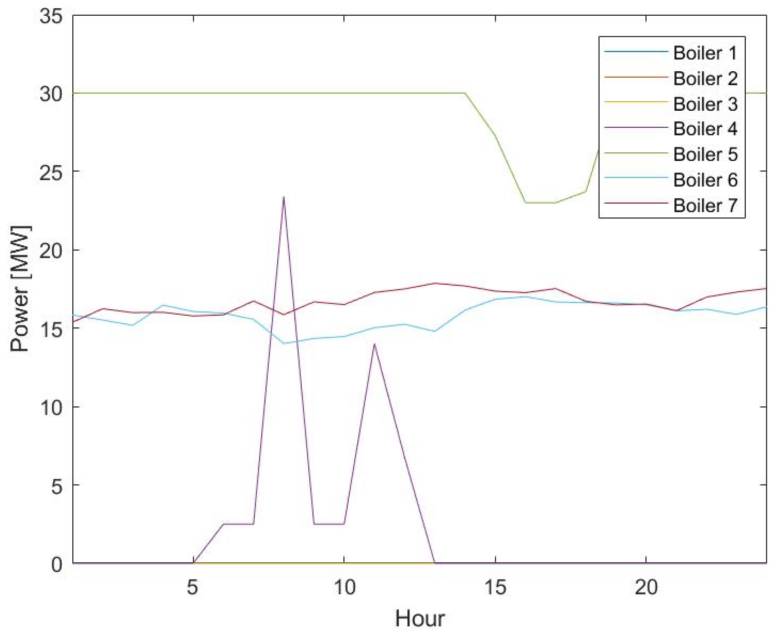

Figure 5.11: Heat load of the boilers at facility 8 on 01.04.2016

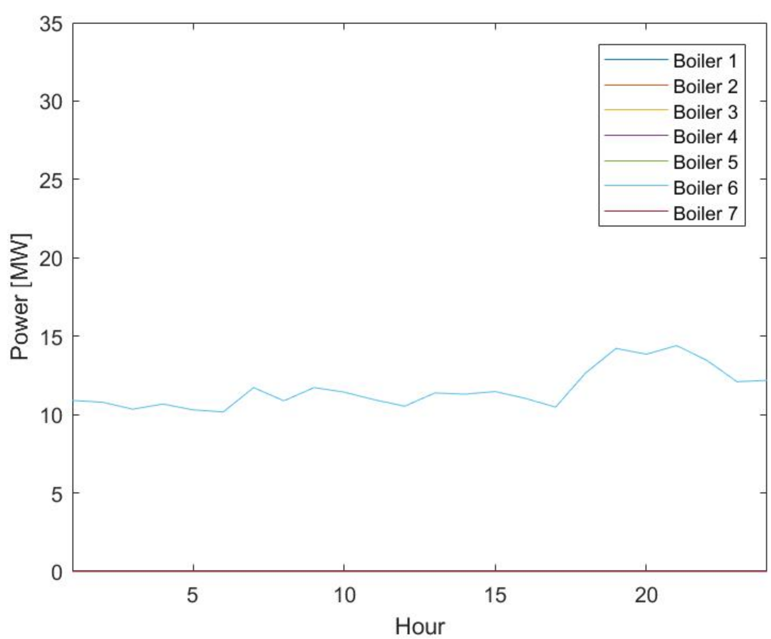

Figure 5.12: Heat load of the boilers at facility 8 on 01.07.2016

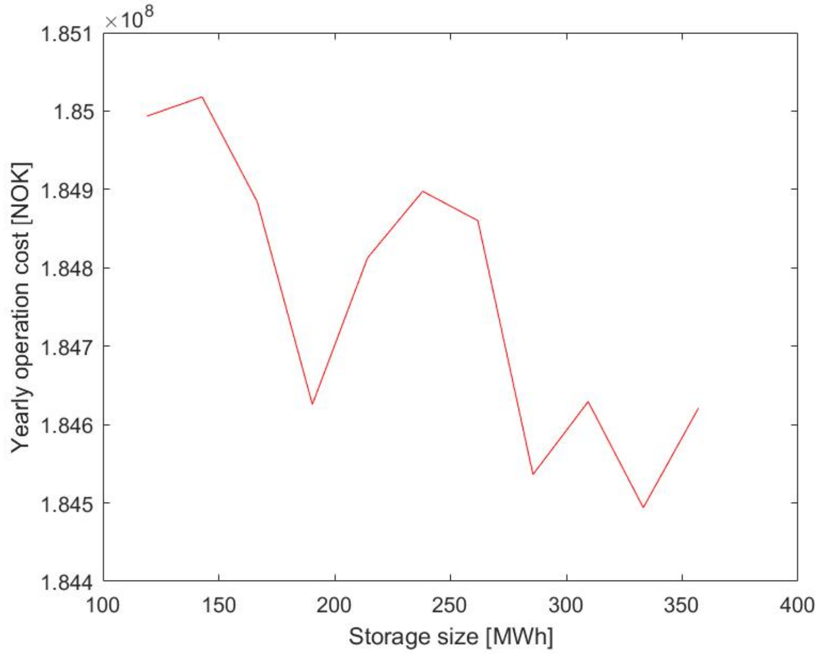

Figure 5.13: Sensitivity analysis of thermal energy storage size

5.3.2 Sensitivity Analysis

Dependency of Yearly Operation Cost on Thermal Energy Storage Size

To better understand the effect of different parameters on the yearly cost, a sensitivity analysis has to be performed. When investigating the economic viability of a TES, the most pressing issue is deciding its size. This can be done by comparing the cost savings achieved with different TES sizes. Figure 5.13 shows the results of performing a sensitivity analysis based on storage size.

It is interesting to note that the yearly operation cost is not strictly decreasing with TES size. The reason is, apparently, that the genetic algorithm is a stochastic method which will generally not acquire the same result twice. There are more possibilities for cost savings, when the TES size is larger, but the algorithm may not always find the best solutions. The random nature of the algorithm means that it can find extraordinarily many optimal solutions on one run of simulations, while fewer optimal solutions are found on the next run.

This is problematic in regards to the confidence of the results. As the figure is based on only one simulation per data point, it is probable that the optimal costs have not been found, so the dependence shown in the figure is not a proven relationship.

Increasing TES size seems to generally affect the yearly cost in the negative direction. This is to expected. One point, in particular, breaks with this pattern. That is the point where the storage size is 190 MWh. The yearly operation cost in that point is 186,200,000 which is considerably lower than the operation costs with TES capacities of 214 MWh, 238 MWh and 262 MWh. Since a larger TES size only increases possibilities, and does not limit them, the optimal solutions with a larger TES is at least as good as previous solutions with smaller TES. Because of that fact, the conclusion must be that, by random chance, more optimal solutions were found when using a TES size of 190 MWh.

Another interesting point, is that the relationship between storage size and yearly operation cost seems to flatten as TES sizes become larger. It is reasonable, since one is expanding the TES into an area of diminishing returns. This is illustrated well by figure 5.1. A storage size of 286 MWh is enough to eliminate a relative daily variation of 6.1%. When summing the relative daily variation under a horizontal line drawn from 6.1%, one finds the total amount of daily variations eliminated by the TES. Overall, it is enough to eliminate 79% of daily variations, and has a utilization of 66%. Increasing the TES size any further would only have minor benefits in reducing daily variations, but with a substantial decrease in utilization.

Dependency of Yearly Operation Cost on Thermal Energy Storage Heat Load Capacity

The yearly operational cost versus HL capacity of the TES, is plotted in figure 5.14. It is evident that the yearly operational cost is more sensitive to changes in HL capacity than to changes in TES size, since the difference between the maximum and minimum costs are 500,000 NOK for TES size and 1,300,000 NOK for HL capacity.

Savings of 340,000 NOK can be made by increasing the HL capacity from 9.5 MW to 13.3 MW. From that point onwards, the dependency seems to flatten out. As is the case with TES size, there is an area of diminishing returns.

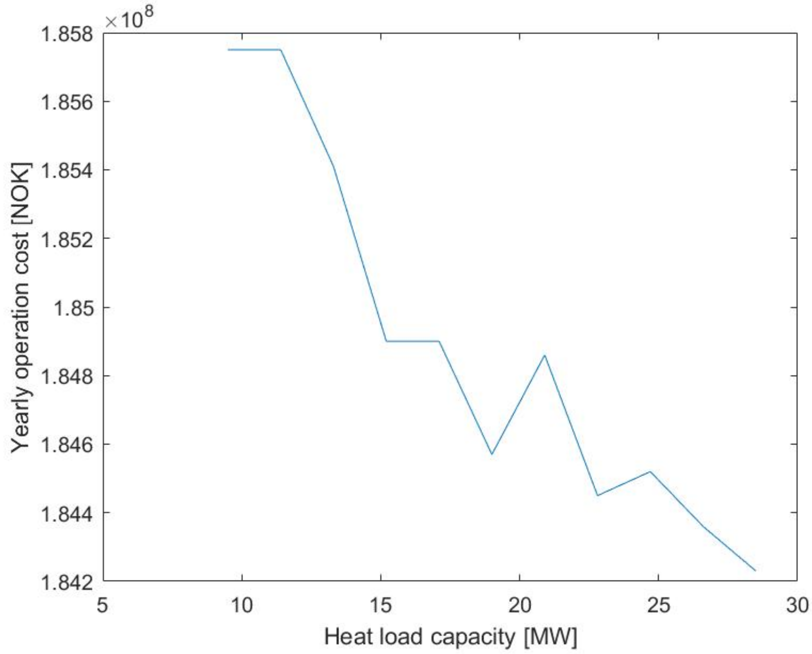

Figure 5.14: Sensitivity analysis of thermal energy storage heat load capacity

When increasing HL capacity, one should be wary of the effect it has on the discharge efficiency ratio. Higher water speeds will be required to achieve the highest HL capacities, so that more turbulence is created in the tank. This, in turn, promotes mixing in the tank, so that the tank can not be run equally efficiently. Such effects are not included in the sensitivity analysis, but they must be accounted for when selecting HL capacity. It is possible with the proposed framework, to make a sensitivity analysis regarding discharging efficiency ratio as well.

Running one sensitivity analysis with 11 simulations, takes around 26 to 32 hours on an AMD Ryzen 5 1600 processor. If one is planning to use the framework for comprehensive sensitivity analyses based on tens of parameters, powerful hardware is required.

Chapter 6

Concluding Remarks and Recommendations for Further Work

Two working models for heat load prediction have been developed. Their performance in predicting the heat load demand for Oslo's district heating grid on an hourly basis have been compared. Their performances were tested by predicting the heat load from 2013 to 2014. Comparisons showed that out of the two models, the one using MLR had the least spread errors, and was therefore deemed more effective overall.

Additionally, a model for solving the unit commitment problem, and performing load dispatch, has been developed. It was based on the genetic algorithm, using a simple priority list method to dispatch the load at each hour. An advantage of the model, is that it can perform simulations with a TES installed as well. This was used to investigate the profitability of adding an accumulator tank to the system. The results showed that a system with an accumulator tank can save 1.3 million NOK yearly, based on simulations performed on data from 2016. The investment in a tank is not profitable, given an assumed cost of 39 million NOK.

Future work on prediction models will aim at getting more accurate predictions. When it comes to the MLR model, it had problems achieving precise predictions in the border areas, where the dependency of HL on outdoor temperature is not linear. This is true in the area where temperatures are getting so low that the heating equipment of the customers are already turned up to the maximum.

When it comes to the neural network, predicted HL was more scattered from the measured HL. This can mainly be attributed to the fact that it uses fewer input parameters than the MLR. However, if one tries to add more relevant parameters to the model, one risks adding a lot of irrelevant information to model, since past values of all added parameters are simultaneously added as well. To achieve increased precision with a RNN, one has to use a different kind of RNN, that does not have to take in past values of all the input parameters. One could for example use a similar RNN to the one used by Kato et al. (2008).

A weakness in both models, is that they do not include all of the relevant input parameters. In particular, predictions on holidays were shown to have large errors. This issue could be negated by including such data in the models.

When it comes to the model for operational optimization, it is very flexible and can be used for systems of different sizes, or over longer planning horizons. It is possible that optimizing for longer planning horizons can lead to more optimal operation of the TES. The reason for this is that, generally, no energy will be saved from one day to the next, as the model can not see that far into the future.

A strength of the model, is that it does not require a smooth cost function. This makes it able to work well on a highly complex search space like a unit commitment problem.

A weakness of the model, is that it is based on randomness, so that the optimality of the solutions can not be guaranteed. To ensure the validity of the results, one would have to perform multiple simulations, which can be very time consuming when simulating operation over longer periods. When optimizing one day at a time, however, the running time is not an issue.

Another term that would be possible to include in the cost function, is the variation of boiler efficiencies with part load. For this study, only constant efficiencies were acquired, so they are the ones that were used. In the future it would be interesting to study the relationship between part load and efficiency, if such data is available. If so, a function describing this relationship can be included in the model.

Additionally, other operation expenses could be added, if one acquires relationships between the HL of the boilers, and such expenses is known. For example, a thought scenario where one knows the pumping cost as a function of boiler HL, would be possible to study.

Appendix A

Acronyms

DH District heating

FAC2 Factor of two

FB Fractional bias

HL Heat load

LNG Liquefied natural gas

MAPE Mean average percentage error

MG Geometric mean bias

MLR Multiple linear regression

NMSE Normalized mean square error

R Correlation coefficient

RNN Recurrent neural network

TES Thermal energy storage

VG Geometric mean variance

Bibliography

Aanensen, T. and Fedoryshyn, N. (2014). Fjernvarme og fjernkjøling i norge utvikling i sentrale størrelser.

Bahnfleth, W. P. and Musser, A. (1998). Thermal performance of a full-scale stratified chilled-water thermal storage tank. *ASHRAE transactions*, 104:377.

Carrion, M. and Arroyo, J. M. (2006). A computationally efficient mixed-integer linear formulation for the thermal unit commitment problem. *IEEE Transactions on Power Systems*, 21(3):1371–1378.

Chang, J. and Hanna, S. (2004). Air quality model performance evaluation. *Meteorology and Atmospheric Physics*, 87(1-3):167–196.

Cheng, C.-P., Liu, C.-W., and Liu, C.-C. (2000). Unit commitment by lagrangian relaxation and genetic algorithms. *IEEE Transactions on Power Systems*, 15(2):707–714.

Cohen, A. I. and Sherkat, V. R. (1987). Optimization-based methods for operations scheduling. *Proceedings of the IEEE*, 75(12):1574–1591.

Damousis, I. G., Bakirtzis, A. G., and Dokopoulos, P. S. (2004). A solution to the unit-commitment problem using integer-coded genetic algorithm. *IEEE Transactions on Power Systems*, 19(2):1165–1172.

Dasgupta, D. and McGregor, D. (1994). Thermal unit commitment using genetic algorithms. *IEE Proceedings - Generation, Transmission and Distribution*, 141(5):459–465.

Diaconescu, E. (2008). The use of narx neural networks to predict chaotic time series. *WSEAS TRANSACTIONS on COMPUTER RESEARCH*, 3(3):182–191.

Dotzauer, E. (2002). Simple model for prediction of loads in district-heating systems. *Applied Energy*, 77:277–284.

Dotzauer, E. (2003). Experiences in mid-term planning of district heating systems. *Energy*, 28(15):1545 – 1555.

Gadd, H. and Werner, S. (2013). Daily heat load variations in swedish district heating systems. *Applied Energy*, 106:47–55.

Gil, E., Bustos, J., and Rudnick, H. (2003). Short-term hydrothermal generation scheduling model using a genetic algorithm. *IEEE Transactions on Power Systems*, 18(4):1256–1264.

Graver, S. (2016). Akkumulatortank skal gi mer miljøvennlig avfallsvarme i trondheim. http://www.energi.no/akkumulatortank-skal-gi-mer-miljovennlig-avfallsvarme-i-trondheim. [Accessed: 13.06.2018].

Gross, G. and Galiana, F. D. (1987). Short-term load forecasting. *Proceedings of the IEEE*, 75(12):1558–1573.

Idowu, S., Saguna, S., Åhlund, C., and Schelén, O. (2014). Forecasting heat load for smart district heating systems: A machine learning approach. pages 554–559.

Kato, K., Sakawa, M., Ishimaru, K., Ushiro, S., and Shibano, T. (2008). Heat load prediction through recurrent neural network in district heating and cooling systems. pages 1401–1406.

Kazarlis, S. A., Bakirtzis, A. G., and Petridis, V. (1996). A genetic algorithm solution to the unit commitment problem. *IEEE Transactions on Power Systems*, 11(1):83–92.

Lourakis, M. I. (2005). A brief description of the levenberg-marquardt algorithm implemented by levmar. *Foundation of Research and Technology*, 4(1):1–6.

Ma, Z., Li, H., Sun, Q., Wang, C., Yan, A., and Starfelt, F. (2014). Statistical analysis of energy consumption patterns on the heat demand of buildings in district heating systems. *Energy and Buildings*, 85(Supplement C):464 – 472.

Magnus Dahl, Adam Brun, G. B. A. (2017). Decision rules for economic summer-shutdown of production units in large district heating systems. *Applied Energy*.

Maifeld, T. T. and Sheble, G. B. (1996). Genetic-based unit commitment algorithm. *IEEE Transactions on Power Systems*, 11(3):1359–1370.

MathWorks. Least squares fitting. https://se.mathworks.com/help/curvefit/least-squares-fitting.html. [Accessed: 20.12.2017].

MathWorks. narxnet. https://se.mathworks.com/help/nnet/ref/narxnet.html. [Accessed: 21.12.2017].

MathWorks. nlinfit. https://se.mathworks.com/help/stats/nlinfit.html. [Accessed: 24.11.2017].

MathWorks. Shallow neural network time-series prediction and modeling. https://se.mathworks.com/help/nnet/gs/neural-network-time-series-prediction-and-modeling.html. [Accessed: 27.12.2017].

Nord Pool. Historical market data. https://www.nordpoolgroup.com/the-power-market/Day-ahead-market/. [Accessed: 01.03.2018].

Nord Pool. Historical market data. https://www.nordpoolgroup.com/historical-market-data/. [Accessed: 24.11.2017].

NVE (2015). Vannkraft. https://www.nve.no/energiforsyning-og-konsesjon/vannkraft/. [Accessed: 06.03.2018].

Ouyang, Z. and Shahidehpour, S. M. (1991). An intelligent dynamic programming for unit commitment application. *IEEE Transactions on Power Systems*, 6(3):1203–1209.

Rosvold, K. A. and Vinjar, A. (2015). kraftutveksling med utlandet. `https://snl.no/kraftutveksling_med_utlandet`. [Accessed 19.07.2018].

Sakawa, M., Kato, K., and Ushiro, S. (2002). Operational planning of district heating and cooling plants through genetic algorithms for mixed 0–1 linear programming. *European Journal of Operational Research*, 137(3):677 – 687.

Sakawa, M., Kato, K., Ushiro, S., and Inaoka, M. (2001). Operation planning of district heating and cooling plants using genetic algorithms for mixed integer programming. *Applied Soft Computing*, 1(2):139 – 150.

Senjyu, T., Shimabukuro, K., Uezato, K., and Funabashi, T. (2003). A fast technique for unit commitment problem by extended priority list. *IEEE Transactions on Power Systems*, 18(2):882–888.

Sharma, A., Tyagi, V. V., Chen, C., and Buddhi, D. (2009). Review on thermal energy storage with phase change materials and applications. *Renewable and Sustainable energy reviews*, 13(2):318–345.

Swarup, K. S. and Yamashiro, S. (2002). Unit commitment solution methodology using genetic algorithm. *IEEE Transactions on Power Systems*, 17(1):87–91.

Thakur, N. and Titare, L. S. (2016). Determination of unit commitment problem using dynamic programming. *International Journal of Novel Research in Electrical and Mechanical Engineering*, 3(1):24–28.

Thomsen, P. and Overbye, P. (2016). Energy storage for district energy systems. In *Advanced District Heating and Cooling (DHC) Systems*, pages 145–166. Elsevier.

Verda, V. and Colella, F. (2011). Primary energy savings through thermal storage in district heating networks. *Energy*, 36(7):4278 – 4286.

Wang, H., Yin, W., Abdollahi, E., Lahdelma, R., and Jiao, W. (2015). Modelling and optimization of chp based district heating system with renewable energy production and energy storage. *Applied Energy*, 159(Supplement C):401 – 421.